Materials Reports: Energy xxx (xxxx) xxx

Contents lists available at ScienceDirect

Materials Reports: Energy

journal homepage: www.keaipublishing.com/en/journals/materials-reports-energy

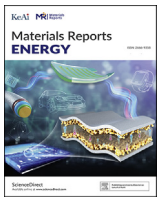

Review

Tailoring solvation sheath for rechargeable zinc-ion batteries: Progress and prospect

Xiaomin Cheng [a], Jing Dong [a], Haifeng Yang [a,f], Xiang Li [c], Xinyu Zhao [a], Bixian Chen [a,f], Yongzheng Zhang [b,*], Meinan Liu [d], Jian Wang [a,e,**], Hongzhen Lin [a,***]

[a] i-Lab & CAS Key Laboratory of Nanophotonic Materials and Devices, Suzhou Institute of Nano-Tech and Nano-Bionics, Chinese Academy of Sciences, Suzhou, 215123, China
[b] State Key Laboratory of Chemical Engineering, East China University of Science and Technology, Shanghai, 200237, China
[c] Anhui Provincial Key Laboratory of Green Carbon Chemistry, Fuyang Normal University, Fuyang, 236037, China
[d] State Key Laboratory of Featured Metal Materials and Life-cycle Safety for Composite Structures, Guangxi Key Laboratory of Processing for Non-Ferrous Metals and Featured Materials, School of Resources, Environment and Materials, Guangxi University, Nanning, 530004, China
[e] Helmholtz Institute Ulm (HIU), D89081 Ulm, Karlsruhe Institute of Technology (KIT), D76021 Karlsruhe, Germany
[f] School of Materials Science and Engineering, Jiangsu University, Zhenjiang, 212013, Jiangsu, China

ARTICLE INFO

Keywords:
Aqueous zinc-metal based batteries
Desolvation
Electrolyte strategy
Interfacial layer

ABSTRACT

Aqueous zinc-metal based batteries (AZMBs) perfectly combine safety, economy and pro-environment, but their performance is arresting limited by the interfacial instability caused by the large desolvation energy barrier of $[Zn(H_2O)_6]^{2+}$ and the massive release of active water at the electrolyte/electrode interface. In this review, we briefly outline the solvation structure of zinc ions and the necessity of desolvation. Subsequently, the variety of strategies to solve these issues, mainly including reorganizing solvation sheath by changing electrolyte environment and accelerating interface desolvation by constructing artificial interfacial layer, are categorically discussed and systematically summarized. Meanwhile, perspectives and suggestions regarding desolvation theories, interfacial evolution, material design and analysis techniques are proposed to design highly stable zinc anodes.

1. Introduction

The immoderate consumption of fossil fuels and the unprecedented degradation of climate urge scholars to explore energy transformation. Developing cost-effective and highly secure energy storage systems is requisite for better utilizing the sustainable clean energy of solar energy, wind energy and hydro energy. As an alternative safe and eco-friendly electrochemical system, zinc-metal based batteries (ZMBs) with aqueous electrolytes have received considerable attention owing to their impressive theoretical capacities (820 mAh g^{-1} or 5855 mAh cm^{-3}) and high natural abundance.[1,2] The rechargeable AZMBs are representatively constituted by the metallic Zn anode, the Zn^{2+} host cathode and the zinc-containing salts electrolyte, which can take place the reversible Zn plating/stripping on the anode and Zn^{2+} insertion/extraction on the cathode to realize the energy storage/release.[3] It is worth noting that rampant dendrite growth, parasitic hydrogen evolution reaction (HER) and chemical corrosion occurring on the Zn surface significantly degrade the output energy density and shorten the actual lifespan of the Zn anode, hindering the commercialization of AZMBs.[4,6]

Based on the current researches, the bottlenecks mentioned above are largely influenced by the interfacial instability, which is a result of the solvation structure of hydrated Zn ions in aqueous electrolyte.[7–9] Specifically, as Zn^{2+} moves from the electrolyte to the anode interior, it experiences the status of hydrated Zn ions in the bulk electrolyte. When it reaches the Helmholtz double layer and loses its solvation shell, Zn^{2+} couples with electrons to form Zn atom and finally grows into the bulk aggregations (Fig. 1a).[10] The geometrical characteristics of electrochemical deposits are mostly governed by the Zn nucleation and growth process, which are highly related to the dehydration process. Firstly, the high desolvation energy barrier of hydrated Zn ions limits the interfacial

* Corresponding author.
** Corresponding author. i-Lab & CAS Key Laboratory of Nanophotonic Materials and Devices, Suzhou Institute of Nano-Tech and Nano-Bionics, Chinese Academy of Sciences, Suzhou, 215123, China.
*** Corresponding author.
E-mail addresses: zhangyongzheng@ecust.edu.cn (Y. Zhang), jian.wang@kit.edu (J. Wang), hzlin2010@sinano.ac.cn (H. Lin).

https://doi.org/10.1016/j.matre.2025.100313
Received 8 October 2024; Received in revised form 1 November 2024; Accepted 7 November 2024
2666-9358/© 2025 The Authors. Publishing services by Elsevier B.V. on behalf of KeAi Communications Co. Ltd. This is an open access article under the CC BY-NC-ND license (http://creativecommons.org/licenses/by-nc-nd/4.0/).

Please cite this article as: Cheng X et al., Tailoring solvation sheath for rechargeable zinc-ion batteries: Progress and prospect, Materials Reports: Energy, https://doi.org/10.1016/j.matre.2025.100313

Table 1
Summary of desolvation strategies for electrolytes.

Electrolyte modifications	Current density	Temperature (°C)	Voltage hysteresis (mV)	Ionic conductivity (mS cm^{-1})	Lifespan (h)	CE (%)	Ref.
30 M $ZnCl_2$	C0.2A0.02	25	13	–	600	95.4	24
7.5 M $ZnCl_2$	C0.2A0.2	−70	176	1.79	450	99.52	40
0.5 M $Zn(ClO_4)_2$ and 18 M $NaClO_4$	C0.2A0.02	25	38	98.5	1200	98.2	26
Trehalose	C5A1	25	48	106.6	1600	99.6	45
Taurine	C1A1	25	31	–	4000	99.9	54
HA+2 M $ZnSO_4$	C1A1	25	50	47.7	5500	99.71	61
50% Sucrose+2 M $ZnSO_4$	C0.5A0.5	25	80	8.27	10000	99.94	31
70% THFA+1 M $Zn(OTf)_2$	C1A1	25	75	20	2750	>99	51
PSCA/$Zn(OTF)_2$	C1A0.5	25	42	–	750	98.4	55
DCZ-gels+1 M $Zn(OTf)_2$	C0.5A0.5	25	45	38.6	2000	99.4	60

C means current density (mA cm^{-2}) and A means deposition capacity (mAh cm^{-2}).

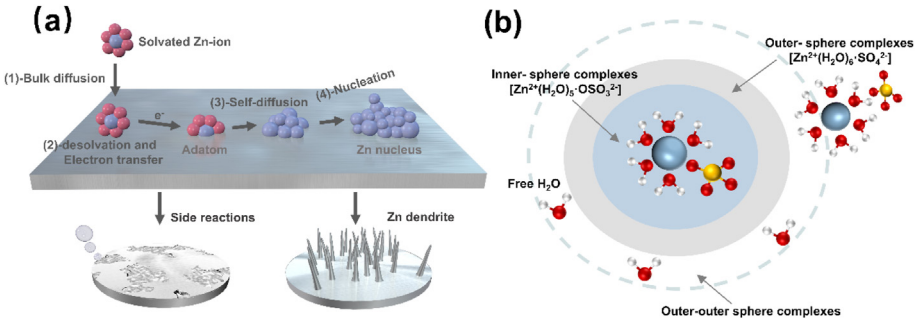

Fig. 1. (a) Schematic diagram of Zn plating. (b) Solvation structure of zinc ions in $ZnSO_4$ electrolyte.

mass transfer kinetics of zinc ions.[11] Especially at low temperatures, the solidification of electrolytes due to the hydrogen bonding network intensifies the coordinate bond between Zn^{2+} and O. This makes the dissociation of the hydrated Zn^{2+} and diffusion of Zn^{2+} more retarded and affects the stability of zinc anode at high charging and discharging depth.[12] Secondly, the solvated H_2O molecules, which are closely coordinated with Zn^{2+}, are more likely to decompose into H^+ and OH^- at the electrode/electrolyte interface during electrodeposition, causing HER and corrosion reactions.[2] The interface environment deterioration arising from side reactions further worsens the reversibility of Zn anode. Thirdly, the mismatch between sluggish desolvation and rapidly coupled electrons causes the speedy depletion of surface Zn^{2+}, inducing the growth of Zn dendrites. In brief, the water-rich solvation structure notably affects the Zn plating/stripping process and deteriorates the stability of Zn anode.[10] How to regulate the solvation structure and control the excessive participation of water molecules in electrodeposition is the key problem that needs to be solved urgently.

To address these issues, extensive efforts are devoted to regulating the solvation structure from the aspects of electrolyte composition regulation to anode surface modification, which can change the solvation shell and regulate the coordination environment of Zn^{2+} in bulk electrolyte via crowding strategy, or accelerate the removal of solvent-water molecules at the electrode/electrolyte interface via functional coating prior to electrodeposition of zinc ions.[13–17] As discussed above, the water-rich solvation structure and sluggish dissociation kinetics from hydrated Zn^{2+} to generate free Zn^{2+} account for the unsatisfactory performances. To date, a great deal of reviews have appeared about the regulation of electrolyte composition and modification of the electrode surface to improve homogeneous Zn deposition and inhibit side reactions. Nevertheless, the methods of implementing desolvation without sacrificing conductivity and how the desolvation kinetics affect electrochemical performance are lacking in summarization.

Herein, we systematically review the development of modulation strategies based on recent advances in the electrolyte and anode toward high-performance AZMBs. First, the solvation structure of Zn^{2+} is briefly reviewed, and we put forward feasible dehydrate strategies, including solvation reorganization and artificial interface layer construction. Second, electrolyte optimization strategies for regulating the solvation shell, such as high-concentration electrolytes, electrolyte additives, and gel electrolytes, are summarized. The regulation mechanism of each strategy is discussed in detail. Third, artificial pre-desolvation mechanisms are proposed based on the artificial layers of MOF/COF, zeolite molecular sieves, inorganic dielectric materials and catalysts. Finally, based on the existing research foundation, the outlook for future development and direction is put forward to consummate the mechanism of desolvation and develop new electrolytes or layers to improve desolvation kinetics and achieve high-performance aqueous AZIBs.

2. Solvation structure and desolvation strategy

2.1. Hydrated zinc ion structure

It is well known that H_2O molecules function as the solvent in ZMBs, which shuttle zinc ions between the Zn anode and cathode and provide an environment for redox reactions, playing a non-negligible role in interface stability.[18] $ZnSO_4$, as a typical electrolyte, has shown the possibility of realizing ZMBs with high energy density owing to its low cost, solvent compatibility, solubility and electrochemical stability.[19] During the dissolution of $ZnSO_4$, Zn^{2+} can combine with six dipolar water molecules via coordinate bonds to solvate in the form of $[Zn^{2+}(H_2O)_6{\cdot}SO_4^{2-}]$ in the 1st solvation shell, while SO_4^{2-} does not appear in the 1st solvation shell of Zn^{2+}. In the 2nd shell, there exist approximately nine water molecules with loosely coordinated bonds and 2.8 SO_4^{2-}, which are further confirmed by molecular dynamics (MD) simulations.[20] It is worth noticing that $[Zn(H_2O)_6]^{2+}$ with high free hydration energy and the dominating H_2O considering the ion-dipole interaction, lead to a high desolvation energy barrier for Zn^{2+} before the deposition process.[21] A good deal of active H_2O released during the desolvation of $[Zn(H_2O)_6]^{2+}$ further aggravates the HER and corrosion reaction, affecting the reversibility and uniformity of Zn^{2+} exchange in liquid and solid phases.

2.2. Desolvation strategy

According to the above analysis of the electrolyte, modulating the solvation structure to reduce the number of combinative water molecules in the 1st solvation shell provides a promising way to improve the stability of Zn anode.[22] Electrolyte optimization by adding functional additives to the electrolyte is the most simple and convenient method to modulate the solvation structure.[23] For example, in highly concentrated zinc salts (e.g., $ZnCl_2$, $Zn(NO_3)_2$ and $Zn(TFSI)_2$) electrolyte, the stronger electrostatic binding force between Zn^{2+} and bulky anions can expel the water molecules around Zn^{2+}.[24–26] With organic solvents as additives in electrolyte, the discrepancy in the capability of functional groups to bind Zn^{2+} or H_2O can weaken the bonding of Zn^{2+}-H_2O and supersede water molecules around Zn^{2+} to a certain extent.[18] Despite reduced water activity via electrolyte optimization, the strong interaction between Zn^{2+} and anions/functional groups results in a high desolvation energy barrier, severely limiting the deposition kinetics.

Apart from the above strategy focusing on modulating the solvation structure, accelerating the dehydration process during electron transfer by constructing an interface layer is another effective strategy to stabilize the Zn anode, inspired by the partially desolvated cations inserted in electrode materials.[27–30] Specifically, by constructing an artificial interface layer with nano-pore structure and specific functional groups on the surface of Zn metal, solvent water molecules are effectively removed before approaching the Zn surface. This method effectively avoids the drawbacks of high viscosity and low ionic conductivity caused by portion electrolyte additives. How to design and select materials with customized sizes and functional groups to enhance the ability of desolvation is an urgent problem.

2.3. Analytical technology of desolvation behaviors

At present, different spectroscopic technologies coupled with theoretical calculations have been used to check the evolution of solvation structure qualitatively in bulk electrolyte, which can reveal specific information about the type and relative content of covalent bond. Specifically, Raman and FTIR spectroscopy can detect the coordination state and relative contents of functional groups in first solvated shell. Detailed relaxation dynamics information of water molecules, including electron migration of Zn^{2+}-OH_2 and the size of solvation shell, can be visualized by nuclear magnetic resonance (NMR) and X-ray absorption spectroscopy (XAS).[31] In addition, density functional theory (DFT) and MD simulation are further conducted to supply the thermodynamic parameters of desolvation energy, binding energy, and HOMO/LUMO, as well as the structural parameters of radial distribution function (RDF) and coordination number (CN), which can further confirm the variation of the solvation structure in the electrolyte.[32,33] However, it is difficult to directly detect the dynamic evolution of hydrated Zn^{2+} in real-time during the electrodeposition process due to the complexity and dynamics of interfacial reactions and the intrinsic characteristics of solvation structure. Interfacial in-situ characterizations should be developed to monitor the real-time interfacial evolution and trace the dynamic variation of coordination bond on solvated clusters in the electrolyte/electrode interface.

3. Solvation shell reconstruction by electrolyte engineering

3.1. Super concentrated electrolytes

In 2015, Suo et al. first reported a highly concentrated aqueous electrolyte, categorized as "water-in-salt electrolyte", by dissolving LiTFSI with extremely high concentrations in water, which inhibits the activity of water and provides expanded electrochemical stability.[34] Subsequently, this strategy was widely used in Li-ion, Na-ion, K-ion and Zn-ion batteries.[24,35,36] As the salt concentration increases, anions are enforced into the solvation sheath structure to form significant ion-pairing, altering the solvation sheath structure of Zn^{2+}. The reduced water reactivity significantly mitigates side reactions and widens the voltage window. At present, various zinc salts, such as $ZnCl_2$,[25] $Na(ClO_4)_2$,[26] $Zn(BF_4)_2$,[37] $Zn(TFSI)_2$,[38] $Zn(Ac)_2$,[5] coupled with lithium, sodium and potassium salts are widely studied. Ji's group developed a high concentration $ZnCl_2$ (30 M) electrolyte and found that more $[ZnCl_4]^{2-}$ appeared whereas the concentration of $[Zn(OH_2)_2Cl_4]^{2-}$ decreased with the $ZnCl_2$ concentration increasing, which may be attributed to the competition between Cl^- and H_2O for positions adjacent to Zn^{2+}(Fig. 2a). Due to the more $[ZnCl_4]^{2-}$, a higher Coulombic efficiency (CE) and wider electrochemical stability window were achieved in the $ZnCl_2$ electrolyte (Fig. 2b–d).[24] Later, they discovered that 30 M $ZnCl_2$ addressed the capacity fading of $Ca_{0.2}V_2O_5{\cdot}0.8H_2O$ cathode (Fig. 2e and f), elevating the onset potential of oxygen evolution potential and capacity (from 296 mAh g^{-1} to 496 mAh g^{-1}).[25] A similar invigoration was also discovered in V_2O_5 using 30 M $ZnCl_2$ electrolyte, reported by Ma and coworkers (Fig. 2g–i).[39] Besides, water-in-salt electrolyte may change the solid-liquid transition temperature (T_t) by disrupting the original hydrogen bond network and have an impact on the low temperature electrochemical performance.[37] Chen et al. explored the relationship between $ZnCl_2$ concentration and T_t. It was found that 7.5 M $ZnCl_2$ electrolyte had the lowest T_t of −114 °C, which can operate from −90 °C to 60 °C with long cycle stability (Fig. 2j–l).[40] Nevertheless, the effectiveness of this strategy is strongly dependent on the concentration of Zn salts. To enhance the solubility of salts, co-salts strategies utilizing multifarious hydrotropic solubilization agents were proposed, such as lithium salts-based electrolytes (4 M $Zn(CF_3SO_3)_2$-2M $LiClO_4$, 1 M $Zn(TFSI)_2$–20 M LiTFSI, 0.5 M $ZnSO_4$-21 M LiTFSI) and acetate-based electrolytes (10 M $Zn(Ac)_2$–15 M KAc, 10 M $Zn(Ac)_2$–24 M urea, 8 M $Zn(Ac)_2$–30 M acetamide), providing a high possibility for reversible Zn plating/stripping.[5,38,41,42]

The addition of large amounts of salt alters the solvated structure of Zn^{2+}, which not only affects the physicochemical properties of electrolytes (i.e., ionic conductivity and electrochemical stability window), but also impacts the desolvation process. Nonetheless, according to the Stokes-Einstein equation and Nernst-Einstein equation, the high viscosity caused by the high concentration of salt is not conducive to the transport of Zn^{2+}.[43] Considering the economic and environmental effects of costly fluorinated metal salts and highly corrosive chlorine-based salts, applying the current water-in-salt electrolytes to large-scale applications is extremely challenging, especially in harsh scenarios such as low-temperature or fast-charging conditions. Thus, neoteric salt-solvent combinations and functional solubilization agents need to be developed to satisfy the needs of a low-cost electrolyte with decent cyclability and low viscosity. Moreover, the dynamic evolution of ion-pairing within the solvation shell during Zn plating/stripping process should be paid more attention to for providing information about desolvation and mass transportation.

3.2. Solvation shell remodeling by hybrid electrolytes

Apart from super concentrated electrolytes, hybridization of aqueous electrolytes with organic compounds are another feasible strategy to pull out the solvated water molecules from the primary solvation shell and rebuild the hydrogen-bond network.[44,45] So far, esters (dimethyl carbonate (DMC), triethyl phosphate (TEP)),[46,47] ethers (1,2-dimethoxyethane (DME), diethyl ether (Et_2O)),[48,49] alcohols (including ethylene glycol (EG), poly(ethylene glycol) (PEG), tetrahydrofurfuryl alcohol (THFA), sorbitol (SBT)),[50–52] and organic salt (benzene sulfonate (SDBS), sodium dodecyl sulfate (SDS))[19,53] are extensively applied as organic additives to build a water-reduced solvation structure to improve reversibility and stability of Zn anode. Organic compounds with high dielectric constant and appropriate molecular size can reorganize the solvation-sheath structure of zinc ions and change T_t by changing the interactions among ions, H_2O and organic compounds. Strong adhesion between Zn and functional groups enables the additives to stick on Zn

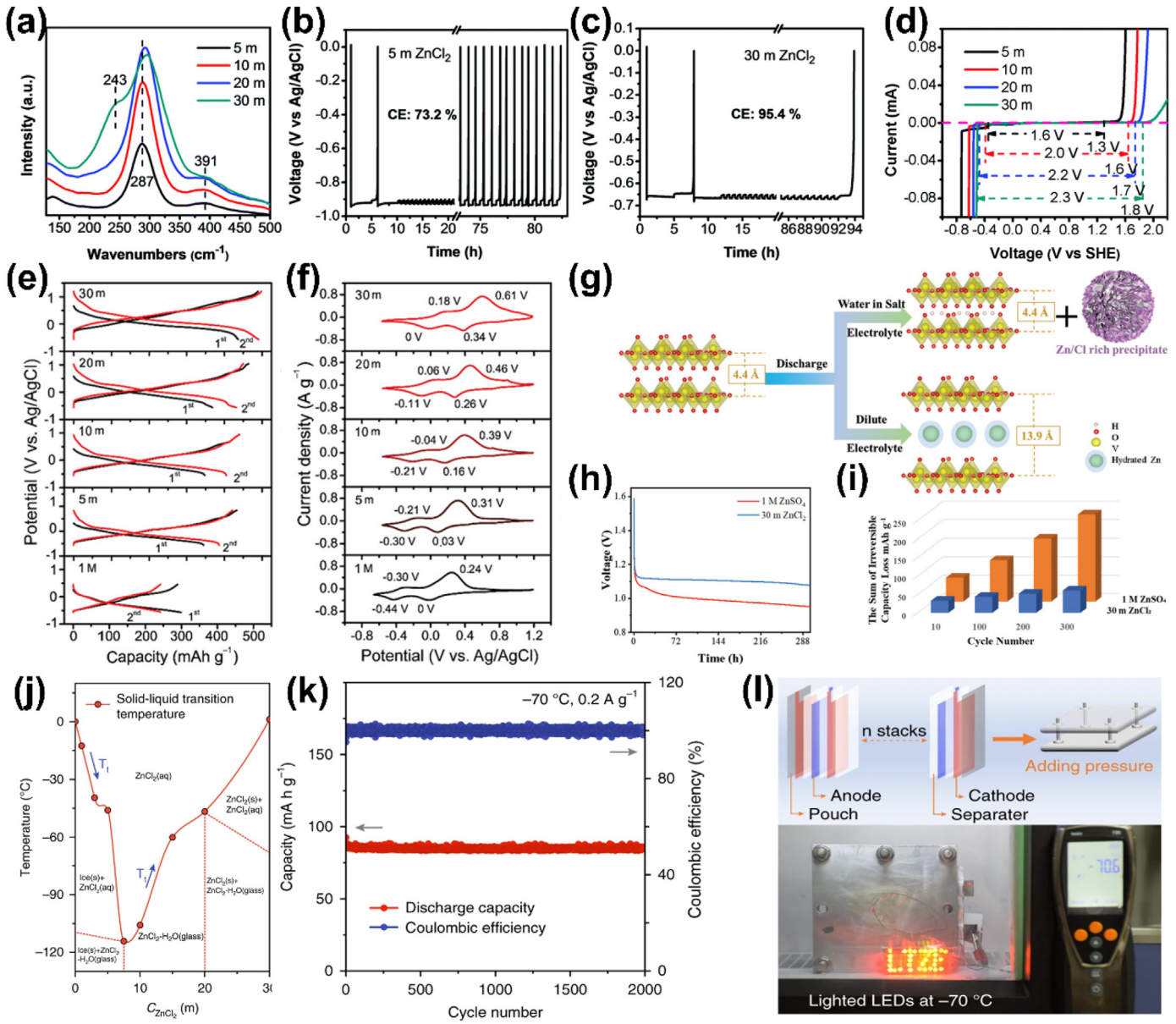

Fig. 2. (a) Raman spectra of various $ZnCl_2$ solutions. CE measurements in symmetric Zn||Zn cells in 5 M (b) and 30 M (c) $ZnCl_2$ electrolyte. (d) LSV curves of the $ZnCl_2$ electrolyte at different concentrations. Reproduced with permission from Ref. 24. (e) GCD potential profiles and (f) *C-V* curves in three-electrode cells. Reproduced with permission from Ref. 25. (g) Schematic illustration of the dynamic structural evolution for V_2O_5 cathode. (h) OCV profiles of V_2O_5 cathode at 55 °C. (i) Sum of irreversible capacity loss during the cycling at 50 mA g^{-1}. Reproduced with permission from Ref. 39. (j) Effect of $ZnCl_2$ concentration on solid-liquid transition temperature. (k) Comparison of long-term cycle stability at −70 °C and 0.2 A g^{-1}. (l) Schematic of assembled pouch cell and photographs of pouch cells for lighting the LED at −70 °C. Reproduced with permission from Ref. 40.

surface, which regulates the interfacial environment to uniform zinc ions. What's more, the additives easily break down to form a stable interfacial layer on both the cathode and anode sides to avoid corrosion reactions and cathode dissolution. Thanks to the synergistic mechanisms mentioned above, water-related side reactions and uncontrollable dendritic Zn are eliminated.

Yang's group utilized tetrahydrofurfuryl alcohol (THFA) as dual hydrogen bond carriers and bidentate ligands in a $Zn(OTf)_2$ aqueous electrolyte to elucidate the ternary solvation clusters.[51] Taking into account viscosity and conductivity, combined with electrochemical properties, 70% THFA content was optimal (Fig. 3a). The interaction between –OH in THFA and the O (C–S=O) formed the hydrogen bonding interactions of –O–H–F–, which caused a red shift in the $–SO_3$ peak, as shown in Fig. 3b, significantly enhancing the participation of OTf^- in the solvation structure. As observed in infrared spectroscopy, the multiple oxygen coordination sites within THFA not only matched up with Zn^{2+} to form a unique bidentate chelation, but also disrupted the hydrogen bonding network among water molecules, inhibiting the reactivity of water. Moreover, the first-principles calculations and in-depth XPS spectra proved the formation of a SEI containing ZnF_2, ZnS and $ZnSO_3$ (Fig. 3c–f). As a result, the Zn||Zn and Zn||VO_2 batteries exhibited stable cycling performance from −40 °C to 60 °C (Fig. 3g and h). Also, $–NH_2$, $–SO_3H$ and $–PO_4$ groups within small organic compounds can ameliorate the interfacial environment by adsorption in IHP to construct a stable SEI and modify Zn^{2+} solvation sheath via interactions between Zn^{2+} and polar groups.[54] For large-sized organic molecules, such as sucrose bio-molecule, it cannot enter the solvation shell due to the steric-hindrance, which is different from the mechanism by participating in the solvation structure. In Chen's report, sucrose featured with hydrogen-bond donors and acceptors weakened the Zn^{2+}-H_2O

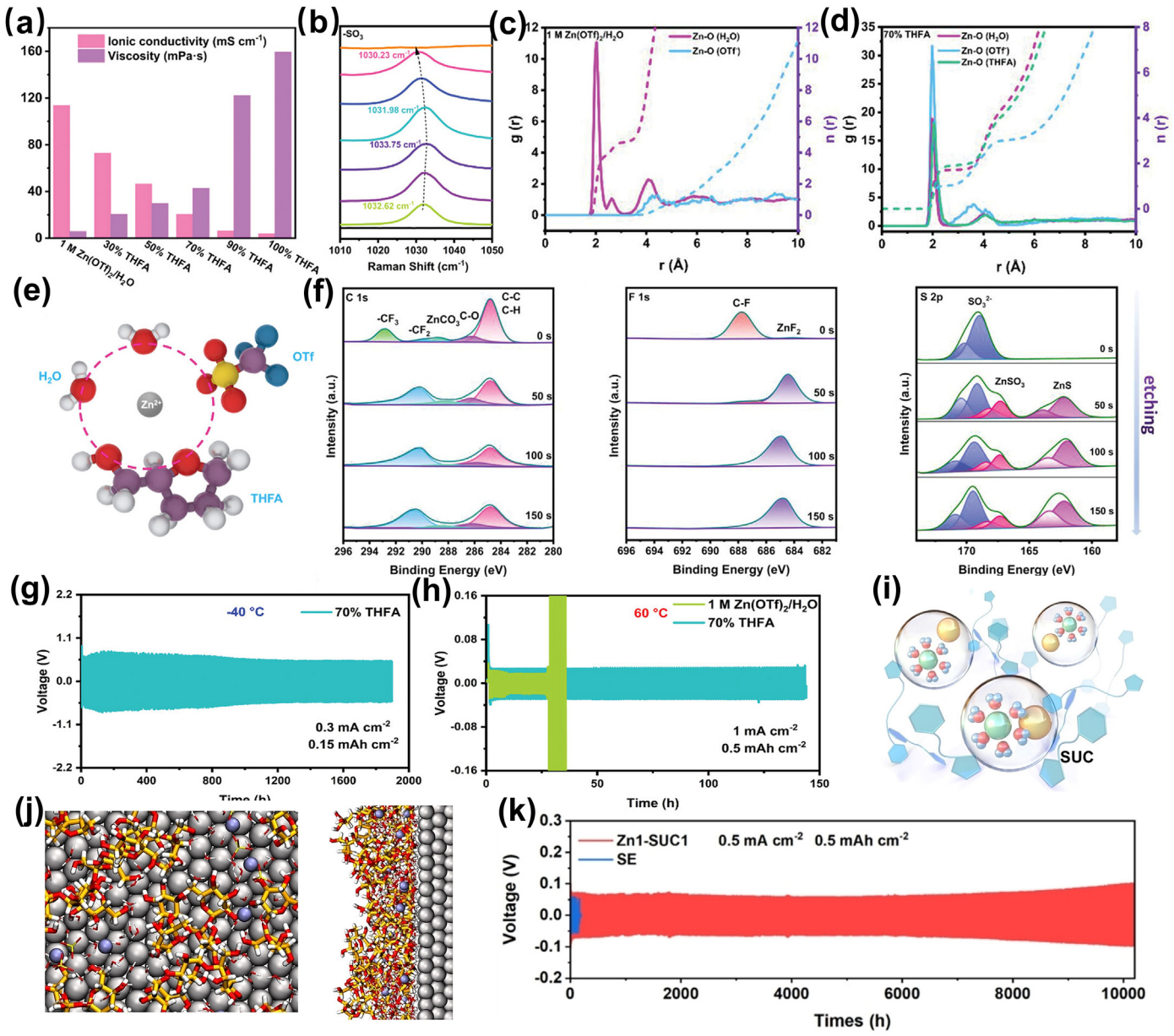

Fig. 3. (a) Summary of the change tendency of viscosity and ionic conductivity. (b) Raman spectra of v-SO_4^{2-} bond. RDF plots in 1 M $Zn(OTf)_2/H_2O$ (c) and 70% THFA electrolyte (d). (e) Possible solvation structure in THFA/$Zn(OTf)_2/H_2O$ electrolytes. (f) In-depth XPS of the cycled Zn anode. (g, h) Galvanostatic Zn plating/stripping in symmetrical cell at −40 °C and 60 °C. Reproduced with permission from Ref. 51. (i) Solvation structure diagram in Zn-SUC electrolyte. (j) Snapshots of MD simulations for Zn1-SUC1. (k) Cycling performance of Zn||Zn symmetrical cells at 0.5 mA cm^{-2}/0.5 mA cm^{-2}. Reproduced with permission from Ref. 31.

interaction, reducing the activity of solvated H_2O and desolvation energy barrier (Fig. 3i).[31] According to MD simulations, sucrose was distributed through the entire EDL, which not only acts as a water-shielding layer to modify the interface chemistry, but also homogenizes the distribution of solvated Zn^{2+} (Fig. 3j). Therefore, the Zn||Zn symmetric batteries delivered an extended operational lifespan exceeding 10000 h at 0.5 mAh cm^{-2} (Fig. 3k).

The functions of organic hybrid electrolyte are multiple, including the interface environment and electrolyte characteristics (T_t, solvation structure and hydrogen-bond network), mitigating Zn metal from water corrosion and endowing AZMBs with versatility toward special environments. Despite the above achievements, the strong interactions between Zn^{2+} and functional groups in primary solvation shell inevitably increase the desolvation energy barrier, resulting in large electrochemical polarization. In addition, most additives participate in interfacial reactions and gradually are consumed, which means that they cannot provide a sustainable effect over a long cycle. The current selection of organic additives is haphazard without consideration of cost-effectiveness and environmental conservation. More attentions are required to explore the effects of different functional groups and molecular sizes on the strength of H-bond network, interaction among the Zn^{2+}, H_2O and polar molecules as well as desolvation ability, putting forward a possible principle to scientifically design functional additives.

3.3. Gel polymer electrolytes

Gel polymer electrolytes embody the polymer matrix, salt mediums and a small amount of water molecules, featuring the three-dimensional network through physical entangling, electrostatic interaction and chemical crosslinking. Compared with liquid electrolytes, gel electrolytes, as quasi-solid substances, have been identified to be effective in alleviating the issues of AZMBs because of the reduced water activity in

their network structure. A wide range of polymer substrates have been employed for the preparation of hydrogel, including polymers such as polyacrylic acid (PAA), polyvinyl alcohol (PVA), polyacrylamide (PAM), and sodium polyacrylate (PAAS), as well as biopolymers such as chitosan, cellulose, chitin, xanthan gum, gelatin, etc. Specific functional groups (e.g., $–NH_2$, –COOH, $–SO_3^-$, –OH, HPO_4^{2-}) embedded in polymer chains have a close affinity with zinc ions or solvated water molecules, which can alter the solvation state of Zn^{2+} and improve the ionic conductivity.[55–59] Besides, ion migration channels constructed by the three-dimensional network endow even and ordered zinc ion transportation, inhibiting the uncontrolled growth of dendrites.

A sustainable cellulose-based hydrogel with abundant -OH groups (DCZ-gel) was designed to modulate the solvation structure of $[Zn(H_2O)_6]^{2+}$, which was reported by Zhou and his colleagues.[60] As illustrated in Fig. 4a, zinc ions preferred being attached by -OH groups on the DCZ-gel backbone rather than water molecules, forming lean-water solvation clusters and facilitating the desolvation process. Guo et al. reported a biocompatible hydrogel electrolyte by utilizing hyaluronic acid (HA), which consists –NH, –OH and $–COO^-$ groups.[61] The ample hydrophilic functional groups provided plentiful bonding sites for H_2O molecules to form HA-H_2O gel, which restricted the water splitting on both cathode and anode sides (Fig. 4c). MD simulations verified that the highly interconnected hydrogen bonds network decreased the average coordination number of H_2O adjacent to Zn^{2+} in HA gel, meaning it reduced the electrostatic interactions between H_2O and Zn^{2+}. Moreover, the negatively charged HA weakened the coordination between SO_4^{2-} and Zn^{2+} by electrostatic repulsion, mitigating SO_4^{2-}-induced corrosion reactions. A distinct increase of free water and a decrease of SO_4^{2-} during the Zn plating process, as well as reversible peak change of H_2O molecule and SO_4^{2-} anion during Zn deposition-dissolution are detected by in-situ synchrotron-FTIR, further confirming the rapid desolvation (Fig. 4d). As a proof of concept, a CE of 99.71% in Zn||Cu cells was realized using HA-H_2O gel and the lifetime of the Zn||Zn cells was extended to 5500 h at 1 mA cm^{-2}/1 mA h cm^{-2} (Fig. 4f). Similar results were found in anionic hydrogel electrolyte, which was constructed by incorporating the $(OSO_3R)^-$ micelles in a cross-linked co-polymer of acrylamide and stearyl

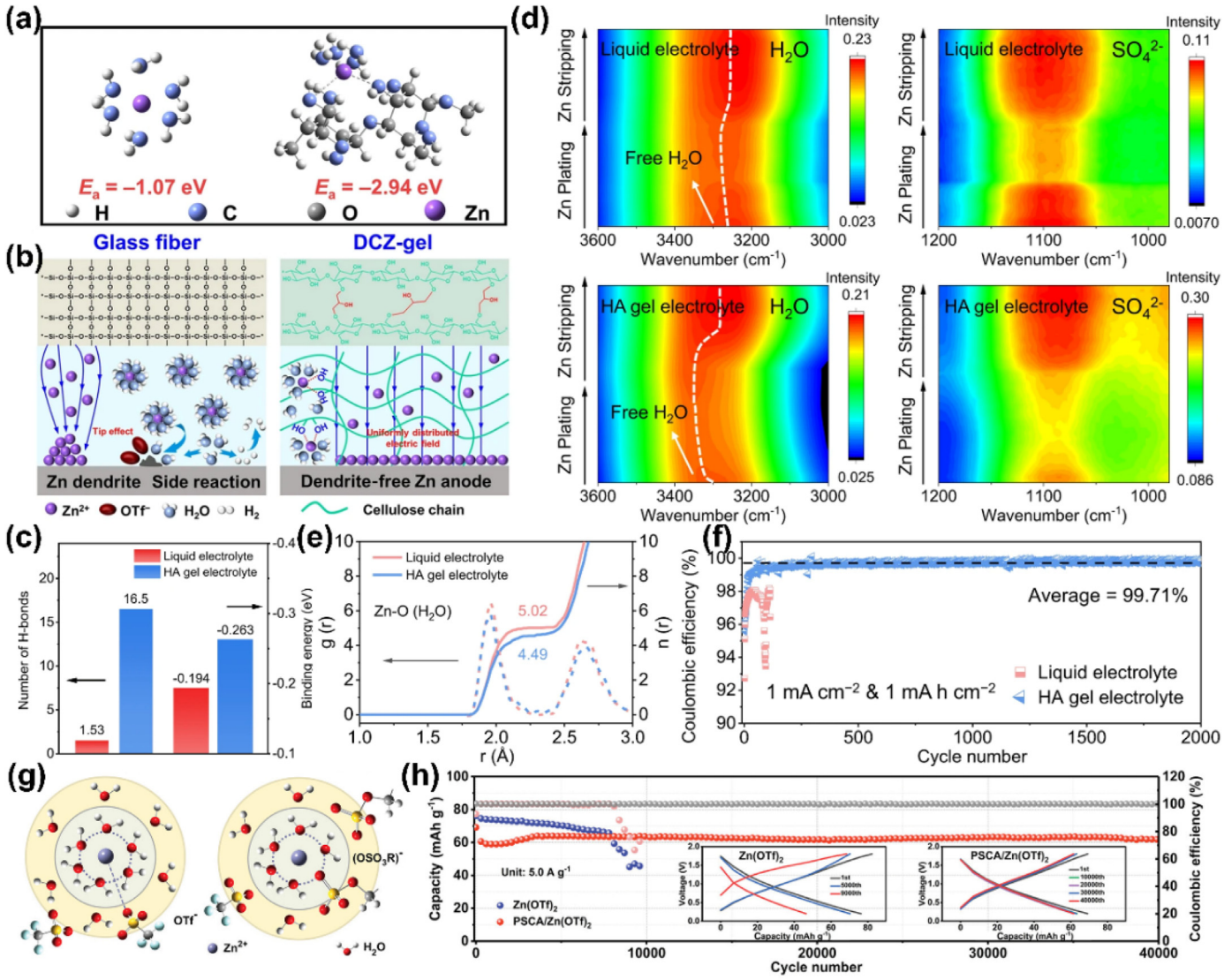

Fig. 4. (a) Binding energy of zinc ion on the $ZnSO_4$ and DCZ-gel electrolytes. (b) Diagram comparing the Zn deposition behaviors by glass fiber and DCZ-gel. Reproduced with permission from Ref. 60. (c) MD simulations of number of H-bond of single H_2O and HA molecule and binding energies of H_2O-H_2O and H_2O-HA. (d) In-situ synchrotron-FTIR spectra in attenuated total reflection (ATR) mode during Zn plating/stripping process to verify desolvation and reversibility. (e) RDF plots in both liquid and HA gel electrolytes conditions. (f) Cycling performance of Zn||Cu asymmetric cells. Reproduced with permission from Ref. 61. (g) Solvation structure in the aqueous electrolyte and PSCA/$Zn(OTf)_2$ hydrogel electrolyte. (h) Galvanostatic charge/discharge curves of Zn||$Zn(OTf)_2$||NPC ZHSC and Zn||PSCA/$Zn(OTf)_2$||NPC ZHSC at 5 A g^{-1}. Reproduced with permission from Ref. 56.

methacrylate.[56] The fixed ionized $(OSO_3R)^-$ micelles could bond with solvated Zn^{2+} and form an average structure of $[Zn^{2+}(H_2O)_{5.73}(OSO_3R)^-_{0.27}]$, as exhibited by the spectroscopic tests and MD simulation (Fig. 4g). Benefiting from this electrolyte, the ion conductivity increased and NPC ZHSC||Zn full cells enabled capacity retention of as high as 89.1% even over 40000 cycles (Fig. 4h).

Different from liquid electrolytes, gel electrolytes continually suffer from low ionic conductivity, poor interface compatibility and insufficient mechanical properties, resulting in a short lifespan and gloomy energy density. Employing inorganic fillers, some zinc salts or a variety of polymers copolymerization to elevate ionic conductivity and mechanical properties is currently the most applied strategy to solve the above-mentioned issues.[62,63] Pan et al. in situ constructed a regulated ion-conductive layer via embedding Si_3N_4 nanoparticles on PVA substrate. Si_3N_4 featured with high dielectric constant results in the space-charge polarization, contributing to the superior ionic conductivity and well-distributed Zn^{2+} flux.[62] Based on the analysis of the gel electrolytes, it is recognized that either the zincophilic functional groups on the polymer chains exert a pull on Zn^{2+} and realize the water exclusion or hydrophilic compounds interlock water molecules to deactivate the water activity. However, whether the anions in the electrolyte participate in the solvation structure and its effects on the subsequent desolvation kinetics have not been clarified. The effect of strong coordination between Zn^{2+} and groups on the electroreduction kinetics of adjusted hydrated Zn^{2+} remains to be further analyzed, guiding the design of hydrogels in turn. At the same time, other functional properties also need to be considered in designing advanced hydrogels, including interface compatibility, mechanical robustness and bio-friendliness.

To sum up, electrolyte composition regulation not only weakens the electrostatic effect between Zn^{2+} and water, and alleviates HER and side reactions, but also expands its application in extreme climates (Table 1). However, the strong coordination between Zn^{2+} and groups leads to the increase of the desolvation energy barrier, which eventually results in the increase of deposition overpotential, damaging the energy density and power density of the battery. In fact, whether in the high concentration electrolyte or the organic additives electrolytes, the optimal suitability among concentration, viscosity and electrochemical performance, as well as cost and environmental impact must be considered. For gel electrolytes, ionic conductivity and interfacial stability are also the great challenges that limit their wide application.

4. Interfacial dehydration accelerated by functional interface layers

The Zn plating and stripping behavior, including $[Zn(H_2O)_6]^{2+}$ dissociation, charge-transfer to form Zn adatoms and subsequently self-diffusion of Zn adatoms, occurs at the electrolyte/electrode interface. Before diffusion and nucleation, the formation of partially desolvated Zn^{2+} at the interface is always not considered by scholars, in spite of which is an essential step in suppressing parasitic side reaction and unifying the Zn^{2+} flux. The huge desolvation energy barrier of $[Zn(H_2O)_6]^{2+}$ must be conquered to improve the Zn^{2+} desolvation kinetics. A straightforward strategy is employed to grab water from the solvated shell of $[Zn(H_2O)_6]^{2+}$ by using a protective coating layer. It is expected that this surface coating acts as a physical buffer layer between zinc anode and electrolyte, effectively inhibiting HER and Zn corrosion during cycling.

4.1. Size-sieving frameworks induced rapid dehydration

Porous materials with customized channels and tunable functional groups have been widely used in gas capture and separation, indicating their potential in the pre-desolvation of different ions. Narrow channels can act as water catchers to trap water molecules from the $[Zn(H_2O)_6]^{2+}$ and promote the formation of an aggregative electrolyte configuration. In this section, the related works on the porous functional interface layer about size-sieving and catalytic desolvation are briefly introduced.

4.1.1. MOFs/COFs

Porous materials, including metal-organic frameworks (MOFs), covalent organic frameworks (COFs) and zeolites, have been shown to prevent the penetration of water onto the Zn anode and suppress the water-induced side reactions, as well as uniform Zn^{2+} flow. When $[Zn(H_2O)_6]^{2+}$ passes through the ordered narrow channels of these porous materials, the difference in size of $[Zn(H_2O)_6]^{2+}$ and channels and the drive of electric field cause water to fall off from the solvated Zn^{2+}, so as to avoid the contact between reactive water molecules and Zn surface. Furthermore, the ordered sub-nano channels of these porous materials can also facilitate highly ordered deposition of Zn^{2+} and enable a dendrite-free Zn metal surface, thereby contributing to Zn metal with high CE and long cycle life. Zhou's group has pioneered the establishment of zeolitic imidazolate framework ZIF-7 coating adhering to the Zn to assess the electrochemical stability (Fig. 5a and b).[64] Raman spectroscopy was applied to check the solvation structure in bulk $ZnSO_4$ electrolyte and ZIF-7 pores. As shown in Fig. 5c, with $ZnSO_4$ electrolyte concentration increasing, the v-SO_4^{2-} band has a significant blue shift, indicating that the hydrated Zn^{2+} gradually transforms from the typical solvation structure of $[Zn(H_2O)_6]^{2+}$ (marked as solvent separated ion pair (SSIP)) to a more close ion association of $[Zn^{2+}(H_2O)_5\ OSO_3^{2-}]$ (named as contact ion pair (CIP)). Obviously, a more constrained $[Zn^{2+}SO_4^{2-}]$ ion association is discovered and the HOH-OH_2 peak is sharply suppressed in the MOF pores, showing the advantage of MOF in regulating desolvation. Under the electric field, large-sized $[Zn^{2+}(H_2O)_6SO_4^{2-}]$ must lose the coordinated water to pass through the size window of ZIF-7, forming a mono-hydrate zinc complex. Benefiting from impeding the penetration of water, the recycled MOF-coated Zn surface is more uniform and there is no by-product accumulation, according to the micro-Raman spectra in Fig. 5d–g. The Zn||Zn symmetric cell can be cycled over 3000 h at 0.5 mA cm^{-2} and the Zn||MnO_2 full cell can deliver a high capacity retention of 88.9% after 600 cycles.

Subsequently, Yang's group used molecular simulations to unveil the dehydration process of solvated Zn^{2+} migrating from bulk electrolyte across the ZIF-7/electrolyte interface into ZIF-7 channels.[20] The results show that the desolvation process is a continuous step-by-step process, and the solvent water molecules can be completely removed with an average of only 10 layers (16 nm) of ZIF-7 (Fig. 5h–j). The homogeneous nucleation of Zn induced by MOF can be explained by the flexibility of MOF with breathing effect. Furthermore, the authors demonstrated that modifying MOF surface with various groups can weaken the Zn^{2+}-H_2O bond and lower the desolvation energy barrier. Given the diversity of MOF and COF and adjustable chemical properties, researchers are devoted to exploring new porous frameworks with multiple function groups anchoring on Zn anode.

Recently, multitudinous MOFs and COFs with functional groups, such as –OH, –F, –SO_3H, –COOH and –NH_2 have been synthesized and acted as an advanced pre-desolvation layer to enhance the stability of Zn anode. Lan and colleagues introduced a series of zincophilic COFs as the protective layer to settle the water-induced side reactions (Fig. 6a).[65] The –C=O/–C=N moieties and suitable pore size of Zn-AAn-COF can repel the H_2O and capture Zn^{2+} within the primary solvation structure according to the electrochemical characterization and theoretical calculations (Fig. 6b), which can efficiently inhibit the HER and achieve dendrite-free morphology. As a result, the PVC-Zn-AAn-COF@Zn symmetric cells can operate over 300 h with low overpotential (< 79.1 mV) at 20 mA cm^{-2} for 1 mAh cm^{-2} (Fig. 6c). A similar tactic was also reported in the study by zhu et al., in which a carboxyl functionalized MOFs (UiO-66-$COOH_2$) are constructed on Zn anode.[66] The –COOH functionalized channels heighten the desolvation process and facilitate ion mobility. Finally, the dendrite-free plating and tiny corrosion from pre-desolvation are achieved (Fig. 6d–g).

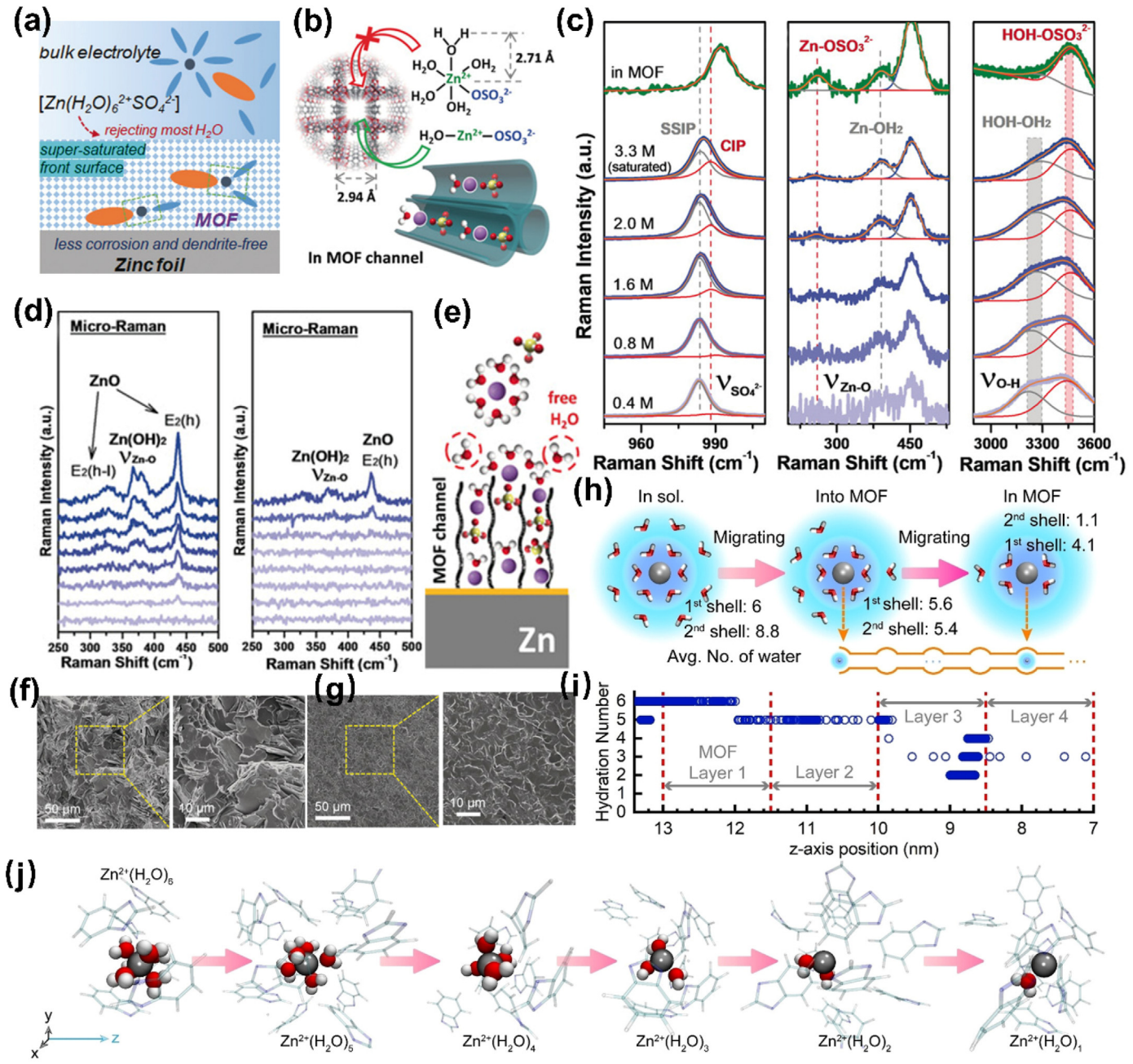

Fig. 5. (a) Schematic diagram of MOF layer constructing a super-saturated front surface. (b) Schematic illustration of function mechanism of MOF channels. (c) Raman spectroscopy. (d) Micro Raman spectroscopy of bare Zn and MOF-coated Zn after cycling at 0.5 mA cm^{-2}. (e) Fast desolvation realized by the MOF layer. SEM images of (f) bare Zn and (g) MOF-coated Zn after 20 cycles. Reproduced with permission from Ref. 64. (h, i) Step-by-step dehydration process along the migration from solution into MOF channel. (j) Snapshots of dehydration process from MD simulation. Reproduced with permission from Ref. 65.

4.1.2. Zeolite molecular sieve and montmorillonite

However, the cumbersome synthesis procedures and high production costs of MOFs/COFs make this strategy depending on them infeasible for large-scale application, which urges researchers to look for other more economical microporous materials. Compared with MOFs and COFs, zeolite molecular sieve is a mature microporous material and has several advantages in terms of production cost, abundance and accessible recyclability, which could make it a competitive candidate for promoting desolvation (Fig. 7a).

Zhou et al. innovatively employed zeolite molecular sieve as a protective coating to study the effect of zeolite molecular sieve on desolvation.[67] Similar to the ZIF-7, both the space confinement endowed by narrow pores and strong interaction bonding between zeolite and H_2O hold the water tightly inside the zeolite, as proved by Raman spectroscopy in Fig. 7b and c. Uniform current field distribution and markedly anti-corrosion capability of zeolite-modified Zn anode are empowered owing to the effective desolvation process, enabling a long cyclic life of Zn||Zn cells (over 4700 h at 0.8 mA cm^{-2}). Subsequently, Fan and co-authors prepared a series of molecular-sieve membranes with different channel dimensions (0.3–11 nm) and investigated the effect of pore size on the ionic environment of Zn^{2+} (Fig. 7d).[68] Channel sizes have a key role in the surface wettability and conductivities, in which the channel size of 5–7 Å is the best, which can be attributed to the size difference (Zn^{2+} (1.48 Å) < 5 Å < $[Zn(H_2O)_6]^{2+}$ (8.6 Å)). As proof, ZSM-5, H-β and Bate membranes with sub-nano channels of about 5–7 Å showed higher surface wettability and smaller energy barriers

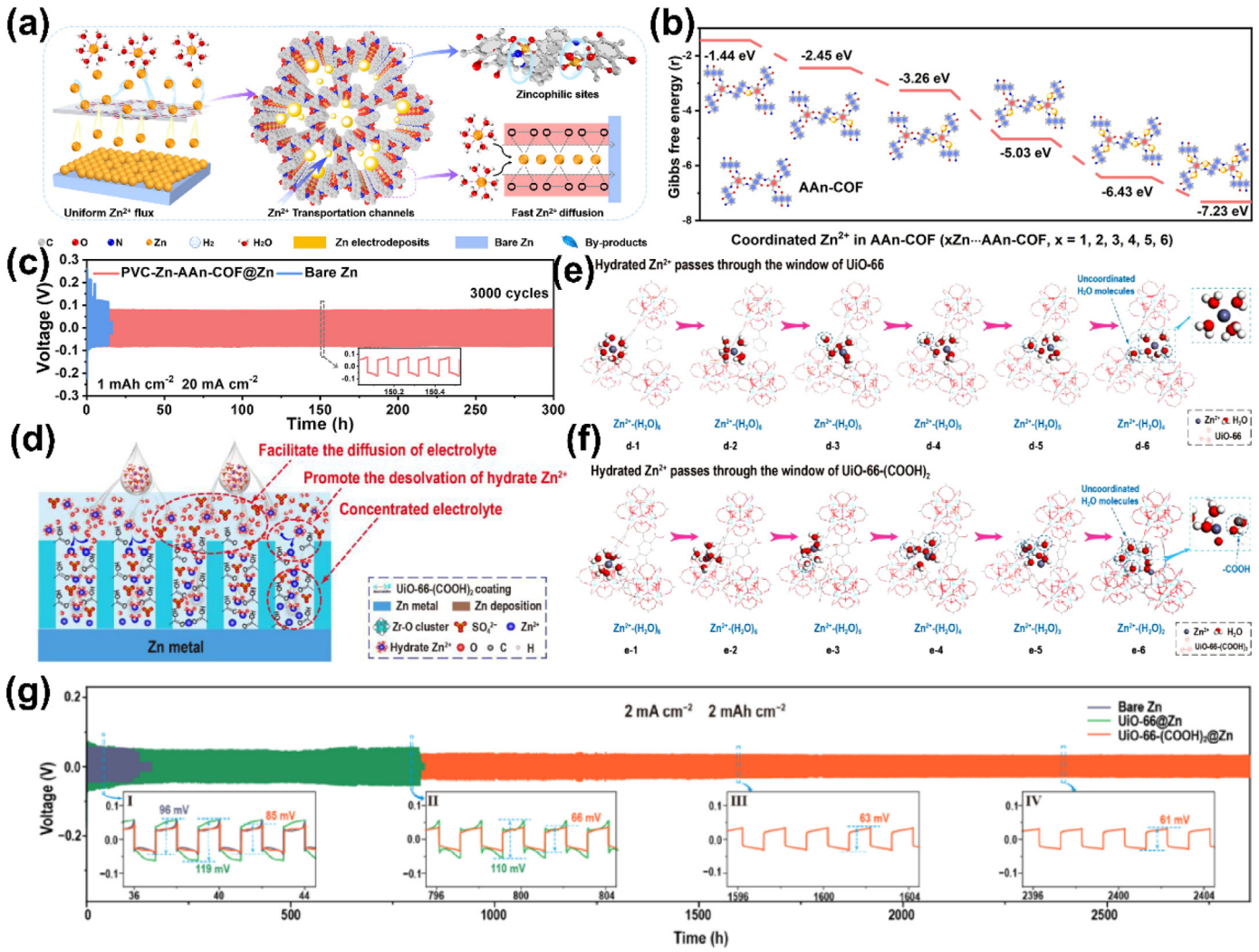

Fig. 6. (a) Schematic diagram of deposition behavior regulated by Zn-COF@Zn. (b) Binding energies of Zn-Aan-COF adsorbing Zn^{2+} with different numbers. (c) Long-term galvanostatic charge and discharge curves at 20 mA cm^{-2}/1 mA cm^{-2}. Reproduced with permission from Ref. 65. (d) Schematic description of desolvation behavior induced by UiO-66-$(COOH)_2$ layer. Comparison the desolvation ability as hydrated Zn^{2+} passes through the window of (e) UiO-66 and (f) UiO-66-$(COOH)_2$. (g) cycling performance at 2 mA cm^{-2}/2 mA cm^{-2}. Reproduced with permission from Ref. 66.

(Fig. 7e–g). This work shows the significance of choosing suitable channel size in realizing Zn^{2+} desolvation. Encouraged by these related works, Wang's group designed a hybrid molecular sieve-based interfacial layer, which combined the advantages of micropores and mesopores in the ZSM-5 and MCM-41 molecular sieves.[69] In addition to increasing the wettability enabled by mesopores, desolvation can also be significantly promoted by the micropores. Consequently, Zn anode with dendrite-free and less H_2 evolution were achieved. Besides molecular sieve, silicate materials such as kaolin, montmorillonite and mullite with structured nanochannels are also used as interfacial protective layers to regulate zinc ions deposition behavior.[70,71] Our group designed a superfast zincophilic ion conductor of layered zinc silicate nanosheet (LZS) to investigate its desolvation behaviors. According to the in-situ sum frequency generation (SFG) spectroscopy, the weaker intensity of O-H band on the Zn@LZS/electrolyte interface after applying 20 mV bias voltage shows the dissociation of $[Zn(H_2O)_6]^{2+}$, providing a firsthand proof to depict the desolvation process (Fig. 7h and i).[7]

In the above literature, the approach for constructing porous materials coating on Zn anode is the traditional doctor blade method, which involves mixing porous materials and binders of polyvinylidene fluoride (PVDF). Yet, this predominant approach has several drawbacks. The PVDF would inevitably occlude the pores of porous materials in the mixing process and numerous tiny cracks would be generated during the evaporation of solvents, resulting in the risk of electrolyte leakage and weakening the desolvation ability. In addition, this method leads to disordered packing of the interlayers, further elongating ion transfer paths and worsening charge transfer resistance. Exploring alternative preparation methods to construct gap-free and ultra-thin porous material layers is a big challenge.

4.1.3. *In situ synthetic porous sieve stratification*

Currently, some researchers have adopted electrochemical-assisted strategies to in-situ construct MOFs/COFs on Zn anode and preliminary results have been achieved.[72] Chao and colleagues have creatively synthesized perforative Janus mesopore SiO_2, which is composed of hydrophilic –OH top layer and hydrophobic –F bottom layer (Fig. 8a).[73] Benefiting from the upper mesopore channels with hydrophilic –OH groups, Zn^{2+} flow at the electrolyte/electrode interface is well-distributed, which was explicitly visualized by color difference via in-situ electrochemical digital holography (EDH) (Fig. 8b). In addition, the Raman spectra and MD simulations proved the tandem chemistry function of hydrophilic-OH and hydrophobic –F Janus channels in the adsorption and desolvation processes of $[Zn(H_2O)_6]^{2+}$ (Fig. 8c and d). Consequently, the Janus channels enable the Zn anode to sustain

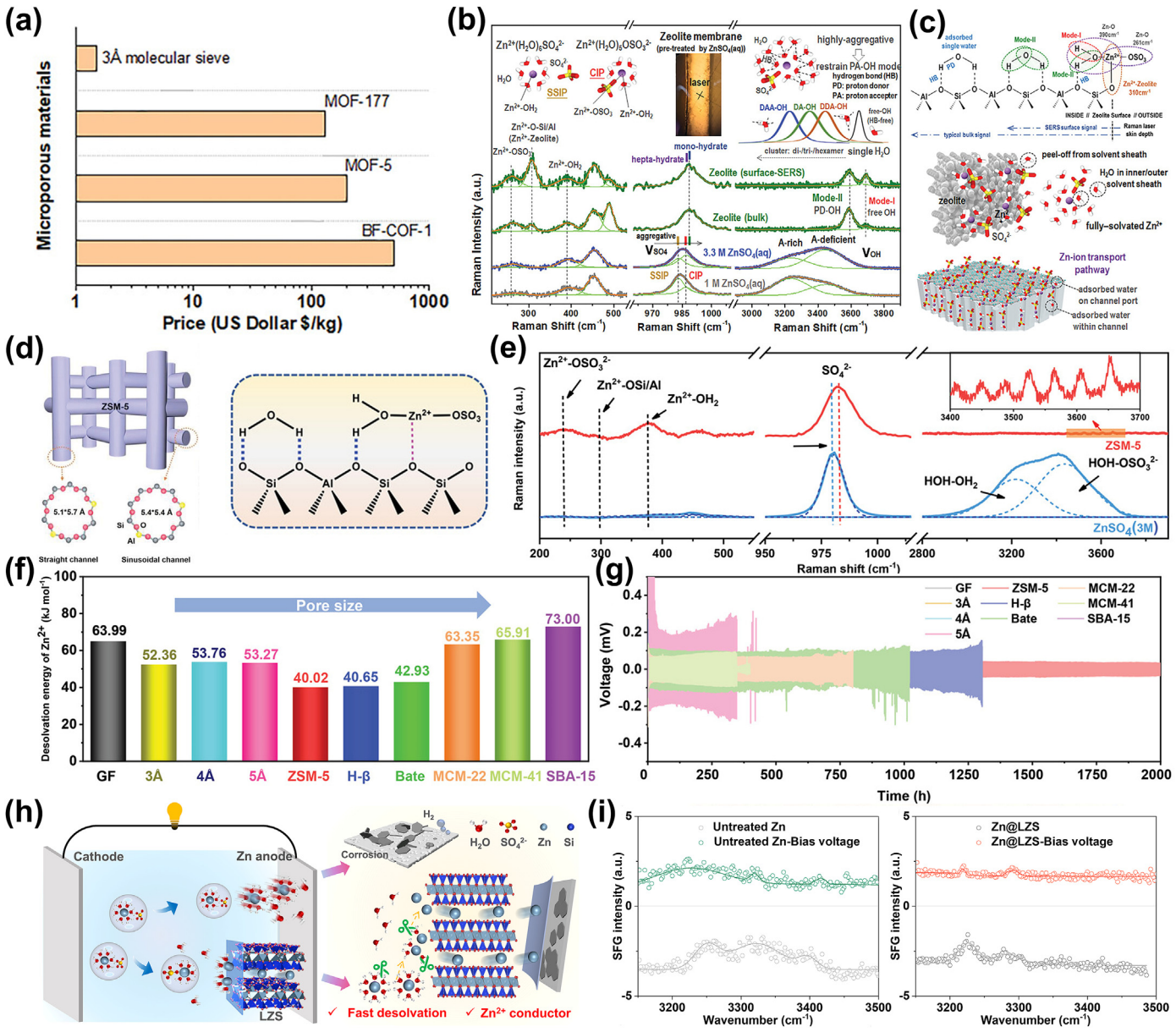

Fig. 7. (a) Comparison of price between molecular sieve and MOFs. (b) Raman spectra of v-SO_4^{2-} and O-H band. (c) Functional mechanism of zeolite on the Zn-ion transport. Reproduced with permission from Ref. 67. (d) Pore structure of ZSM-5. (e) Raman spectra of aqueous $ZnSO_4$ electrolyte. (f) Effect of pore size on the calculated desolvation energy. (g) Cycling performance at 1 mA cm^{-2} for symmetric cells with different molecular sieves layers. Reproduced with permission from Ref. 68. (h) Schematic illustration of the effect of the layered zinc silicate nanosheet on interfacial stability. SFG signal of bare Zn and Zn@LZS before (i) and after throwing the bias voltage of 20 mV (j). Reproduced with permission from Ref. 7.

long-term cycles of 8000 h at 4 mA cm^{-2} (Fig. 8e). Sun et al. for the first time fabricated Co- and Zn-zeolitic imidazolate framework (ZIF-8) interlayers on the Zn foil to fully inherit the advantages of ZIF-8 (Fig. 8f).[74] Based on electrochemical measurements and DFT calculations, fast Zn^{2+} transport kinetic and uniform Zn deposition with less parasitic reactions are realized, which can be attributed to the unimpeded Zn^{2+} transport channels and the affinity of the imidazole ring and Co node within the ZIF-8 structure to Zn (Fig. 8g and h).

As discussed in this section, in-situ constructing an interface with perforative pore structure and polar functional groups can promote the step-by-step desolvation, stripping H_2O from the solvent shell of Zn^{2+} and forming a super-saturated environment. Consequently, it efficiently enhances the kinetics of ion diffusion and mitigates Zn metal free from water corrosion, enabling AZMBs with high cycling reversibility and long lifespan. Despite great accomplishment achieved in in-situ synthesis of MOFs interlayers, only a few types of porous interlayers with single-aperture have been synthesized and the compactness and uniformity of interlayers cannot be guaranteed, limiting further application. In the future, developing hybrid interfaces and exploring novel preparation methods for long-lasting pre-desolvation should pay more attention to strengthening the desolvation capability.

4.2. Rapid interfacial desolvation kinetics accelerated by electronic structure regulation

Apart from relying on the size-sieving function of porous materials to realize desolvation, utilizing the electrical properties of the materials to weaken the covalent bond between Zn^{2+} and solvent H_2O is another strategy to strip H_2O molecules from the solvent shell of Zn^{2+}.

4.2.1. Maxwell polarized electric-field facilitated pre-desolvation

Inorganic dielectric materials can exert spatial charge separation

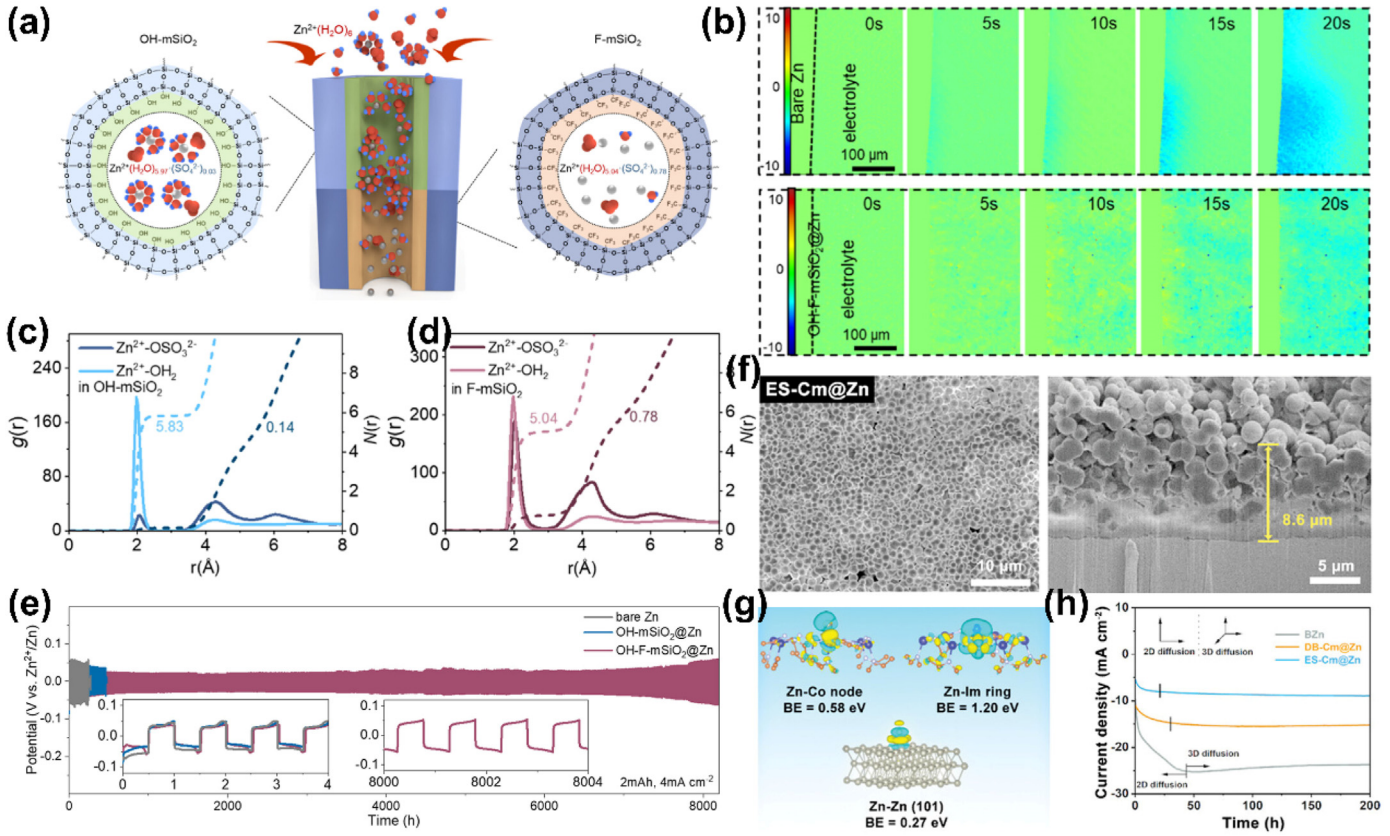

Fig. 8. (a) Mechanism of tandem chemistry inside the Janus mesopores. (b) In situ electrochemical digital holography of bare Zn and OH-F-mSiO$_2$@Zn. (c,d) RDF plots in OH-mSiO$_2$ and F-mSiO$_2$. (e) Cycling performance. Reproduced with permission from Ref. 73. (f) Top-view and cross-sectional SEM images of DB-*Cm*@Zn. (g) Binding energy of Zn on the Co site of ZIF-8, Im ring of ZIF-8 and Zn (101). (h) CA curves. Reproduced with permission from Ref. 74.

between two media with different permittivity and electrical conductivities under an external electric field, which is named as Maxwell Wagner polarization. The Zn metal anode surface can be protected with inorganic materials (e.g., Nb_2O_5, $ZnNb_2O_6$, ZrO_2, HfO_2, $BaTiO_3$), which have been previously demonstrated as effective coating materials. Cao's group combined the advantages of a highly hydrophobic polymer and dielectric $BaTiO_3$ to design a dielectric and hydrophobic organic-inorganic composite coating on Zn surface. They suggested that the hydrophobic interface regulated the desolvation process and $BaTiO_3$ with a high dielectric constant equalized the Zn^{2+} flow.[75] However, the effect of inorganic high dielectric material on the desolvation process is ignored.

Recently, gradually concentrated Zn^{2+} achieved inside $BaTiO_3$ coating with a high dielectric constant was reported by Pan's group.[76] According to Operando Micro-Raman at different positions and depths in the BTO layer, both the v-SO_4^{2-} band and v-HOH-OSO_3^{2-} band shifted significantly to a higher frequency with the depth deepened, which was consistent with the tendency of electrolyte concentrations to increase (Fig. 9a–d). This phenomenon implied that free water molecules gradually decreased and the solvation sheaths were clipped to form aggregative electrolyte when the hydrated zinc ions migrated from the top to the bottom of the BTO layer, suppressing the H_2O-related side reactions. In addition, the aligned dipoles induced electric-field could elicit vertically ordered zinc-ion migration trajectory, unifying Zn^{2+} flow and preventing the formation of dendrites (Fig. 9e). Owing to these properties, the symmetric and asymmetric BTO@Zn cells delivered a long lifespan (1400 h *vs* 82 h), and high Coulombic efficiency (99.9%), as well as a dendrite-free and stable surface (Fig. 8f). Hur's also reported that the Nb_2O_5 layer, in which Lewis acid active sites at Nb atoms can strongly interact with water molecules, promotes the water molecules desolvation from $[Zn(H_2O)_6]^{2+}$, resulting in a rapid Zn-ion transport and reduced side reactions through Nb_2O_5 layer (Fig. 9g).[77] Recently, a dielectric but ion-conductive zinc niobate (ZNB) nanoparticle layer was prepared by Lin's group.[78] Distribution relaxation times (DRT) analyses verified the significant improvement of the ZNB layer on the desolvation (Fig. 9h and i).

Nonetheless, the diffusion kinetics of Zn^{2+} are not obviously optimized, because Zn^{2+} would encounter lattice hindrance when migrating in highly crystalline inorganic dielectric materials. Therefore, obtaining high-speed ion migration channels to foster diffusion kinetics during the Zn plating/stripping process is a challenge for dielectric materials with high crystallinity. Moreover, the function mechanism of aligned dipoles induced electric-field in modulating the solvation structure of zinc ions toward highly stable Zn anode should be further investigated.

4.2.2. *Catalytic desolvation*

As stated in section 2.1, zinc ions combine with six dipolar water molecules via coordinate bond coupling to solvate as the form of $[Zn(H_2O)_6]^{2+}$. The process of desolvation can be regarded as the process of coordinate bonds breaking to generate bare Zn^{2+}. Such features suggest that the desolvation process has similar characteristics to a chemical reaction. Therefore, exploring new-style materials with catalytic function is crucial to the development of desolvation capacity. Understanding the effect of catalyst on improving the zinc ions desolvation and interfacial transfer and deposition kinetics from the perspective of catalytic chemical, and using the design concept of catalyst to guide its structure optimization in turn is necessary.

Liu's group put forward a novel zincophilic/hydrophobic single-atomic asymmetric Zn-$N_{3py+1pr}$-C 3D porous coating via manipulating the electronic interactions between metal and coordination atoms.[79] DFT showed that appropriate metal coordination interaction can well reduce the 3d-band of Zn and form a nonbonding state in the 2p-band of N and C atoms, thus inducing the selective adsorption of Zn^{2+} and weakening the

adsorption of H_2O on the Zn-$N_{3py+1pr}$-C (Fig. 10a–c). The unique "hydrophobic and zincophilic" properties of the Zn-$N_{3py+1pr}$-C were also verified by the contact angle and in-situ optical observations, which obviously suppress the Zn dendrite formation and prolong the cycling performance. Interestingly, the more intensive localized electron state benefitted the H_2O decomposition, which may be detrimental to the desolvation of $[Zn(H_2O)_6]^{2+}$ and the interface stability.

Defect or single-atom materials hold great potential in energy-related applications with the merits of tailoring the atomic structure and high activity, showing enthusiasm ability in enhancing kinetics in electrocatalysis. So far, only a few papers have used defect or single-atom materials as protective layers onto Zn anode. Bi-N_4 moieties fabricated to serve as nucleation seeds to boost Zn nucleation kinetics were reported by Wang's group, in which the single-atomic Bi-N_4 can strongly bond with Zn and guide Zn nucleation (Fig. 10g–j).[80] Li's team incorporated atomically dispersed Cu atoms on g-C_3N_4 to enhance the stability of the g-C_3N_4-based artificial SEI.[81] However, the above works underscore the feasibility of employing single atoms to manipulate nucleation behaviors and ignore the influence of single atoms on the desolvation kinetics, and understanding the mechanism of electron structure modulation promoting desolvation remains a great challenge. Indeed, a trade-off between desolvation activity and hydrogen evolution capacity should be taken into account, and the coverage and failure of the active site during the Zn plating/stripping process are the prospective area for investigation.

5. Summary and further outlook

In conclusion, the interfacial Zn^{2+} desolvation is the prerequisite for successive plating, playing a vital role in inhibiting Zn dendrites and preventing side reactions. We systematically reviewed the solvation structure modulation strategies based on the recent advances in rebuilding the solvation state of Zn^{2+} by electrolyte component regulation and enhancing pre-desolvation by interface layer toward smooth Zn plating without the apparent side reactions. Although partial achievements have been made, a clear and systematic understanding of

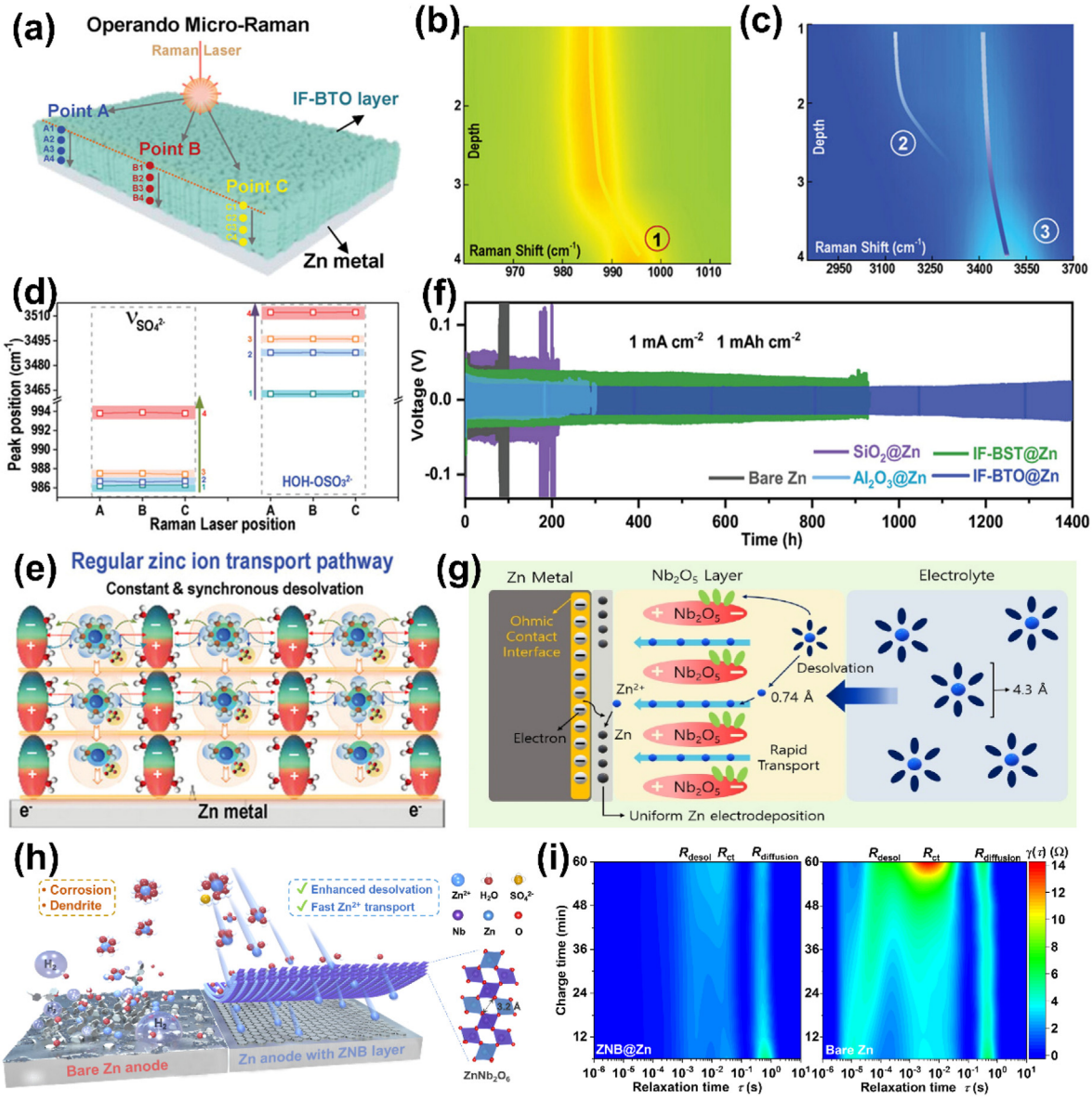

Fig. 9. (a) Schematic illustration of Raman spectroscopy. (b, c) Corresponding Raman spectra inside IF-BTO layer. (d) Comparison of peak positions at different positions and depths. (e) Mechanism of Maxwell polarized electric-field promoting desolvation and ordered migration. (f) Cycling performance of symmetric cells. Reproduced with permission from Ref. 76. (g) Mechanism of promoting zinc ion desolvation induced by Nb_2O_5 layer. Reproduced with permission from Ref. 77. (h) Schematic illustration of ZNB layer for Zn deposition. (i) DRT analysis based Zn||Zn cells during charging process. Reproduced with permission from Ref. 78.

molecular-ions interactions to clarify the mechanism of desolvation is insufficient. Future efforts and considerations toward reducing the desolvation energy barrier are outlined in the following four sections.

5.1. Updating desolvation theories for fast electron/ion kinetics

For the interfacial protective layer, the mechanism of pre-desolvation process can be inspired by physical obstruction and pore size screening coupled with chemisorption, excluding partial H_2O form $[Zn(H_2O)_6]^{2+}$ in the presence of customized size and functional groups. For the electrolyte strategy, water activity is significantly inhibited due to the intricate interactions among Zn^{2+}, H_2O, anions and additives, and electrolyte additives, such as salt, organic molecules, etc., can effectively reduce the amount of solvated water adjacent to Zn^{2+} by crowding strategy. However, the complicated interactions and dynamic interface evolution increase the difficulty of understanding desolvation and even zinc deposition. In particular, the conventional solvation model is proposed based on ambient temperature without considering the effect of low temperature, which may alter interactions within the outer shell and aggravate the difficulty of desolvation. Even if the solvation structure changes, stronger forces need to be overcome at the electrolyte/electrode interface to release Zn^{2+}. As discussed above, the desolvation behaves like a chemical reaction that needs to overcome a high desolvation energy barrier. It is feasible and promising to introduce the idea of catalysis in electrolyte or interface to reduce the desolvation barrier and even change the deposition behavior of Zn^{2+}. Deeper analyses related to information inside the catalyst during cycling need to be employed to further investigate the mechanism of desolvation.

5.2. Revealing the interfacial evolution including Zn^{2+} desolvation, SEI formation and Zn atomdiffusion

Zinc deposition is a complex process that releases solvated water molecules and anions/coordinated species prior to electroreduction. The released coordinated species definitely compete with zinc ions for electrons to preferentially undergo reduction reaction, forming a SEI layer on the zinc surface, changing the PH of the electrolyte and affecting the interface impedance. Subsequently, the composition and structure of SEI have an effect on the longitudinal deposition and transverse diffusion of zinc ions, which will eventually change the deposition morphology. At present, SEI components and zinc ions deposition morphology have been visualized by characterizing the surface of cycled zinc anode, but little information on the dynamic changes of interfacial clusters at the molecular and atomic levels has been available in previous reports. Accurately grasping the desolvation process and redox reactions near the anode surface can establish a relationship between material design and SEI structures, which is of immense assistance in the design and construction of a robust SEI layer.

5.3. Screening reasonable electrolyte or interfacial layers satisfied desolvation and transverse diffusion

The desolvation process to liberate free Zn^{2+} at the electrolyte/electrode interface is the rate-limiting step for Zn deposition due to the strong binding between Zn^{2+} and H_2O molecules, which requires an overwhelming amount of desolvation energy. A delay or inefficiency in the desolvation process can disrupt the Zn^{2+} flux, causing the accumulation

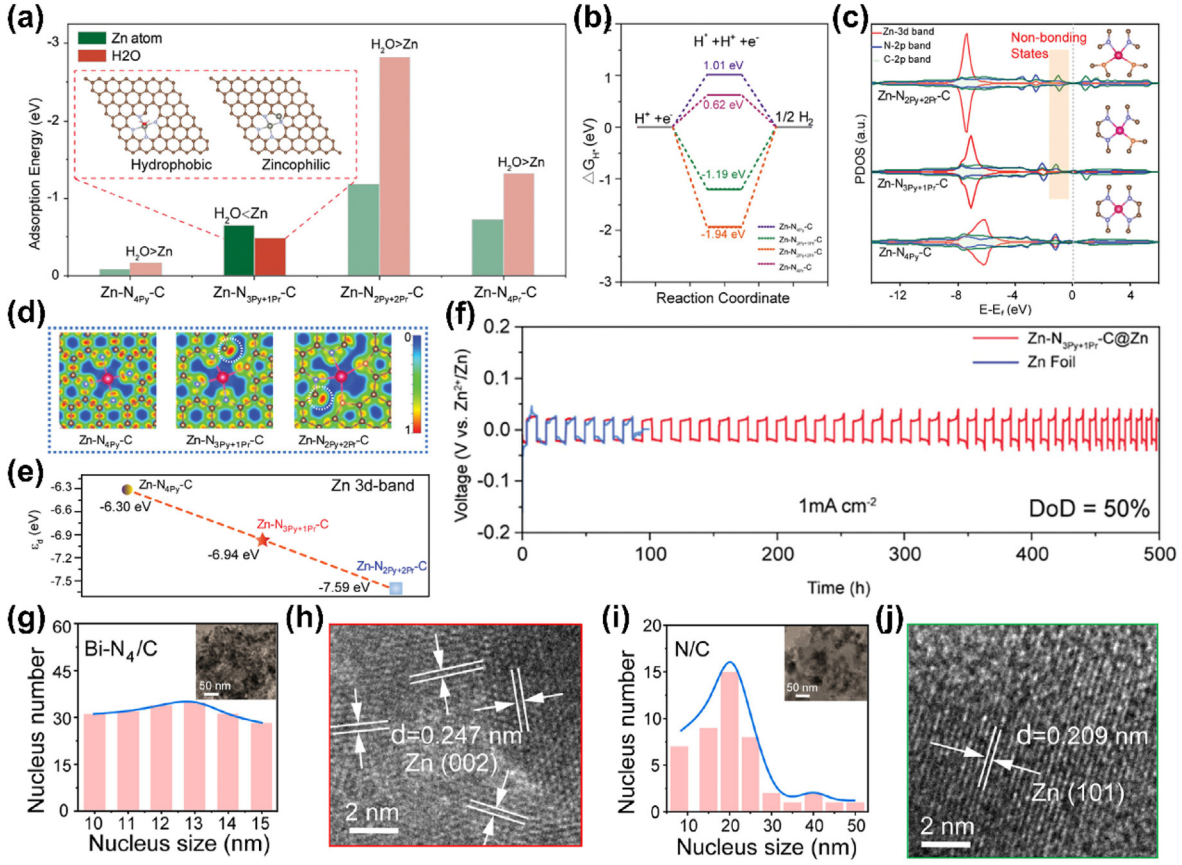

Fig. 10. (a) Comparison of the binding energy of Zn atom and H_2O on different N sites. (b) Calculated H* free energy of Zn-N_4-Cs. (c) PDOS of Zn-N_4-Cs. (d) Electron localization function analysis. (e) 3d-band-center of Zn. (f) Cycling performance of symmetric cells at high DOD. Reproduced with permission from Ref. 79. (g, i) Effect of Bi single atom on Zn deposition behaviors. HR-TEM images of cycled Zn anodes: (h) Bi-N_4/C and (j) N/C layer. Reproduced with permission from Ref. 80.

of H_2O molecules or anions at the electrolyte/electrode interface, contributing to HER and anodic corrosion as well as uneven Zn deposition behavior. Regulatory strategies, including electrolyte composition optimization, hydrogel design, and interfacial layer construction, have been shown to be effective strategies for reducing water activity and enhancing interface stability. However, how to scientifically and purposefully optimize existing materials or design novel materials remains a huge challenge. Combined with the interface evolution, the optimization of SEI components and cathode's compatibility, the element tailoring and electronic structure regulation of additives are a possible research direction. Future investigations should also be devoted to exploiting suitable descriptors to rapidly screen electrolyte additives and interface layers by combining emerging artificial intelligence and machine learning techniques.

5.4. Advanced analysis techniques for tracing (de)solvation and interfacial evolution

Solvation structure is inextricably relevant to the interfacial desolvation and interfacial evolution, which significantly impact the nucleation overpotential and interfacial stability. At present, by means of Raman, FITR and NMR spectroscopy and other conventional testing methods, the static solvation configuration can be obtained. Recently, XAS has been gradually accepted for the characterization of accurate structural information within hydrated Zn^{2+}, including electron density distributions and cluster size. Nevertheless, it is difficult to intuitively and effectively monitor the real-time interfacial evolution and trace the dynamic variation of coordination bonds on solvated clusters in the electrolyte/electrode interface because of its complexity and dynamic nature using the existing characterization methods. Therefore, interfacial in-situ characterizations, such as Operando Micro-Raman, in-situ electrochemical digital holography (EDH), in-situ synchrotron-FTIR and in-situ sum frequency generation (SFG) spectroscopy, should be vigorously developed to uncover the interfacial evolution and dynamic changes of interactions among the Zn^{2+}, H_2O and additives/coatings. Furthermore, DFT calculation and MD simulation are also indispensable, which can not only acquire the reason for the change of solvation structure but also verify the distinct parameters of reorganized solvation structures, such as binding energy, RDF, CN and diffusion energy. In the future, in situ characterization techniques coupled with theoretical simulation toward detecting dynamic interface evolution is an inevitable tendency.

CRediT authorship contribution statement

Xiaomin Cheng: Writing – review & editing, Writing – original draft, Visualization, Validation, Supervision, Project administration, Investigation, Formal analysis, Data curation, Conceptualization. **Jing Dong:** Data curation. **Haifeng Yang:** Data curation. **Xiang Li:** Data curation. **Xinyu Zhao:** Data curation. **Bixian Chen:** Data curation. **Yongzheng Zhang:** Writing – review & editing, Validation. **Meinan Liu:** Data curation. **Jian Wang:** Writing – review & editing. **Hongzhen Lin:** Writing – review & editing, Resources.

Declaration of competing interest

The authors declare that they have no known competing financial interests or personal relationships that could have appeared to influence the work reported in this paper.

Acknowledgements

This work was financially supported by the National Key Research and Development Program of China (2021YFA1201503), National Natural Science Foundation of China (No. 21972164, 22279161, and 22309144), the Natural Science Foundation of Jiangsu Province (BK. 20210130), Shanghai Sailing Program of China (23YF1408900), China Postdoctoral Science Foundation (No. 2024M762318, 2023M731084, and 2023M732561), Suzhou Science and Technology Plan project (SYC2022057), Innovative and Entrepreneurial Doctor in Jiangsu Province (JSSCBS20211428), and Opening funding from Key Laboratory of Engineering Dielectrics and Its Application (Harbin University of Science and Technology) (No. KFM202507, Ministry of Education). Dr. J. Wang thanks the funding provided by the Alexander von Humboldt Foundation. Dr. Y. Zhang thanks the Shanghai Super Postdoctoral Incentive Program. The authors also thank the support from Nano-X, Suzhou Institute of Nano-tech and Nano-bionics, Chinese Academy of Sciences.

References

1. Guo X, He G. Opportunities and challenges of zinc anodes in rechargeable aqueous batteries. *J Mater Chem A*. 2023;11:11987–12001.
2. Yang W, Yang Y, Yang H, et al. Regulating water activity for rechargeable zinc-ion batteries: progress and perspective. *ACS Energy Lett*. 2022;7:2515–2530.
3. Wang Y, Xie J, Luo J, et al. Methods for rational design of advanced Zn-based batteries. *Small Methods*. 2022;6:2200560.
4. Yang H, Yang Y, Yang W, et al. Correlating hydrogen evolution and zinc deposition/dissolution kinetics to the cyclability of metallic zinc electrodes. *Energy Environ Sci*. 2024;17:1975–1983.
5. Dong D, Wang T, Sun Y, et al. Hydrotropic solubilization of zinc acetates for sustainable aqueous battery electrolytes. *Nat Sustain*. 2023;6:1474–1484.
6. Ma W, Wang S, Wu X, et al. Tailoring desolvation strategies for aqueous zinc-ion batteries. *Energy Environ Sci*. 2024;17:4819–4846.
7. Cheng X, Zuo Y, Zhang Y, et al. Superfast zincophilic ion conductor enables rapid interfacial desolvation kinetics for low-temperature zinc metal batteries. *Adv Sci*. 2024;11:2401629.
8. Zhang Q, Zhi P, Zhang J, et al. Engineering covalent organic frameworks toward advanced zinc-based batteries. *Adv Mater*. 2024;36:2313152.
9. Wang T, Wang P, Pan L, et al. Stabling zinc metal anode with polydopamine regulation through dual effects of fast desolvation and ion confinement. *Adv Energy Mater*. 2023;13:2203523.
10. Chang Z, Yang H, Qiao Y, et al. Tailoring the solvation sheath of cations by constructing electrode front-faces for rechargeable batteries. *Adv Mater*. 2022;34:e2201339.
11. Zhou Y, Li G, Feng S, et al. Regulating Zn ion desolvation and deposition chemistry toward durable and fast rechargeable Zn metal batteries. *Adv Sci*. 2023;10:e2205874.
12. Jia L, Hu H, Cheng X, et al. Toward low-temperature zinc-ion batteries: strategy, progress, and prospect in vanadium-based cathodes. *Adv Energy Mater*. 2023:2304010.
13. Zhang W, Dong Q, Wang J, et al. Failure mechanism, electrolyte design, and electrolyte/electrode interface regulation for low-temperature zinc-based batteries. *Small Methods*. 2023;7:e2300324.
14. Zhang Y, Cao Z, Liu S, et al. Charge-enriched strategy based on MXene-based polypyrrole layers toward dendrite-free zinc metal anodes. *Adv Energy Mater*. 2022;12:2013979.
15. Cao J, Zhang D, Zhang X, et al. Strategies of regulating Zn^{2+} solvation structures for dendrite-free and side reaction-suppressed zinc-ion batteries. *Energy Environ Sci*. 2022;15:499–528.
16. Ma G, Yuan W, Li X, et al. Organic cations texture zinc metal anodes for deep cycling aqueous zinc batteries. *Adv Mater*. 2024;36:2408287.
17. Qiu K, Ma G, Wang Y, et al. Highly compact zinc metal anode and wide-temperature aqueous electrolyte enabled by acetamide additives for deep cycling Zn batteries. *Adv Funct Mater*. 2024;34:2313358.
18. Yan H, Zhang X, Yang Z, et al. Insight into the electrolyte strategies for aqueous zinc ion batteries. *Coord Chem Rev*. 2022;452:214297.
19. Yang X, Zhou Q, Wei S, et al. Anion additive integrated electric double layer and solvation shell for aqueous zinc ion battery. *Small Methods*. 2024;8:2301115.
20. Jiang Y, Wan Z, He X, et al. Fine-tuning electrolyte concentration and metal–organic framework surface toward actuating fast Zn^{2+} dehydration for aqueous Zn-ion batteries. *Angew Chem Int Ed*. 2023;62:e202307274.
21. Wu T, Hu C, Zhang Q, et al. Helmholtz plane reconfiguration enables robust zinc metal anode in aqueous zinc-ion batteries. *Adv Funct Mater*. 2024;34:2315716.
22. Han M, Li TC, Chen X, et al. Electrolyte modulation strategies for low-temperature Zn batteries. *Small*. 2023:e2304901.
23. Ma G, Di S, Wang Y, et al. Zn metal anodes stabilized by an intrinsically safe, dilute, and hydrous organic electrolyte. *Energy Storage Mater*. 2023;54:276–283.
24. Zhang C, Holoubek J, Wu X, et al. A $ZnCl_2$ water-in-salt electrolyte for a reversible Zn metal anode. *Chem Commun*. 2018;54:14097–14099.
25. Zhang L, Rodríguez-Pérez IA, Jiang H, et al. $ZnCl_2$ "Water-in-salt" electrolyte transforms the performance of vanadium oxide as a Zn battery cathode. *Adv Funct Mater*. 2019;29:1902653.
26. Zhu Y, Yin J, Zheng X, et al. Concentrated dual-cation electrolyte strategy for aqueous zinc-ion batteries. *Energy Environ Sci*. 2021;14:4463–4473.
27. Zhao H, Fu Q, Yang D, et al. In Operando synchrotron studies of NH^{4+} preintercalated $V_2O_5{\cdot}nH_2O$ nanobelts as the cathode material for aqueous rechargeable zinc batteries. *ACS Nano*. 2020;14:11809–11820.

28. Tian X, Zhao Q, Zhou M, et al. Synergy of dendrites-impeded atomic clusters dissociation and side reactions suppressed inert interface protection for ultrastable Zn anode. *Adv Mater*. 2024:2400237.
29. Fu M, Zhao Q, Long K, et al. Global "Interface-space" dual-modulation by functional supramolecules organic frameworks on aqueous zinc-ion batteries. *Adv Funct Mater*. 2023:2311680.
30. Liu M, Yuan W, Ma G, et al. In-situ integration of a hydrophobic and fast-Zn^{2+}-conductive inorganic interphase to stabilize Zn metal anodes. *Angew Chem Int.* 2023; 62:e202304444.
31. Dou H, Wu X, Xu M, et al. Steric-hindrance effect tuned ion solvation enabling high performance aqueous zinc ion batteries. *Angew Chem Int Ed*. 2024;63:e202401974.
32. Xu W, Li J, Liao X, et al. Fluoride-rich, organic–inorganic gradient interphase enabled by sacrificial solvation shells for reversible zinc metal batteries. *J Am Chem Soc*. 2023;145:22456–22465.
33. Deng W, Xu Z, Wang X. High-donor electrolyte additive enabling stable aqueous zinc-ion batteries. *Energy Storage Mater*. 2022;52:52–60.
34. Suo L, Borodin O, Gao T, et al. "Water-in-salt" electrolyte enables high-voltage aqueous lithium-ion chemistries. *Science*. 2015;350:6263.
35. Liu T, Liu K-T, Wang J, et al. Achievement of a polymer-free KAc gel electrolyte for advanced aqueous K-Ion battery. *Energy Storage Mater*. 2021;41:133–140.
36. Liu T, Du X, Wu H, et al. A bio-inspired methylation approach to salt-concentrated hydrogel electrolytes for long-life rechargeable batteries. *Angew Chem Int Ed.* 2023; 62:e202311589.
37. Sun T, Yuan X, Wang K, et al. An ultralow-temperature aqueous zinc-ion battery. *J. Mater. Chem. A*. 2021;9:7042–7047.
38. Wang F, Borodin O, Gao T, et al. Highly reversible zinc metal anode for aqueous batteries. *Nat Mater*. 2018;17:543–549.
39. Tang X, Wang P, Bai M, et al. Unveiling the reversibility and stability origin of the aqueous V_2O_5-Zn batteries with a $ZnCl_2$ "Water-in-salt" electrolyte. *Adv Sci*. 2021;8: 2102053.
40. Zhang Q, Ma Y, Lu Y, et al. Modulating electrolyte structure for ultralow temperature aqueous zinc batteries. *Nat Commun*. 2020;11.
41. Olbasa BW, Huang CJ, Fenta FW, et al. Highly reversible Zn metal anode stabilized by dense and anion-derived passivation layer obtained from concentrated hybrid aqueous electrolyte. *Adv Funct Mater*. 2021;32:2103959.
42. Zhao J, Li Y, Peng X, et al. High-voltage Zn/LiMn0.8Fe0.2PO4 aqueous rechargeable battery by virtue of "water-in-salt" electrolyte. *Electrochem Commun*. 2016;69:6–10.
43. Khan Z, Kumar D, Crispin X. Does water-in-salt electrolyte subdue issues of Zn batteries? *Adv Mater*. 2023;35:e2300369.
44. Bai S, Huang Z, Liang G, et al. Electrolyte additives for stable Zn anodes. *Adv Sci*. 2023:e2304549.
45. Liu H, Xin Z, Cao B, et al. Polyhydroxylated organic molecular additives for durable aqueous zinc battery. *Adv Funct Mater*. 2023:2309840.
46. Miao L, Wang R, Di S, et al. Aqueous electrolytes with hydrophobic organic cosolvents for stabilizing zinc metal anodes. *ACS Nano*. 2022;16:9667–9678.
47. Zhu J, Yang M, Hu Y, et al. The construction of binary phase electrolyte interface for highly stable zinc anodes. *Adv Mater*. 2023;36:2304426.
48. Deng L, Xie X, Song W, et al. Realizing highly stable zinc anode via an electrolyte additive shield layer and electrochemical in-situ interface. *Chem Eng J*. 2024;488: 151104.
49. Wang X, Wang B, Lei P, et al. Polycation-regulated hydrogel electrolytes with nanoscale hydrophobic confinement inducing Zn(002) deposition for highly reversible zinc anodes. *Energy Environ Sci*. 2024;17:6640–6655.
50. Yang Y, Guo S, Pan Y, et al. Dual mechanism of ion (de)intercalation and iodine redox towards advanced zinc batteries. *Energy Environ Sci*. 2023;16:2358–2367.
51. Qiu Y, Zheng X, Zhang R, et al. Boosting zinc-ion batteries with innovative ternary electrolyte for enhanced interfacial electrochemistry and temperature-resilient performance. *Adv Funct Mater*. 2023:2310825.
52. Qiu M, Sun P, Wang Y, et al. Anion-trap engineering toward remarkable crystallographic reorientation and efficient cation migration of Zn ion batteries. *Angew Chem Int Ed*. 2022;61:e202210979.
53. Xie W, Zhu K, Jiang W, et al. Highly 002-oriented dendrite-free anode achieved by enhanced interfacial electrostatic adsorption for aqueous zinc-ion batteries. *ACS Nano*. 2024;18:21184–21197.
54. Duan G, Wang Y, Luo B, et al. Taurine-mediated dynamic bridging strategy for highly stable Zn metal anode. *Energy Storage Mater*. 2023;61:102882.
55. Lin P, Cong J, Li J, et al. Achieving ultra-long lifespan Zn metal anodes by manipulating desolvation effect and Zn deposition orientation in a multiple cross-linked hydrogel electrolyte. *Energy Storage Mater*. 2022;49:172–180.
56. Guo G, Ji C, Mi H, et al. Zincophilic anionic hydrogel electrolyte with interfacial specific adsorption of solvation structures for durable zinc ion hybrid supercapacitors. *Adv Funct Mater*. 2023;34:2308405.
57. Hu Y, Wang Z, Li Y, et al. Sulfonated hydrogel electrolyte enables dendrite-free zinc-ion batteries. *Chem Eng J*. 2024;479:147762.
58. Feng D, Jiao Y, Wu P. Proton-reservoir hydrogel electrolyte for long-term cycling Zn/PANI batteries in wide temperature range. *Angew Chem Int Ed.* 2022;62:e202215060.
59. Ji S, Qin J, Yang S, et al. A mechanically durable hybrid hydrogel electrolyte developed by controllable accelerated polymerization mechanism towards reliable aqueous zinc-ion battery. *Energy Storage Mater*. 2023;55:236–243.
60. Zhang H, Gan X, Yan Y, et al. A sustainable dual cross-linked cellulose hydrogel electrolyte for high-performance zinc-metal batteries. *Nano-Micro Lett*. 2024;16:106.
61. Li G, Zhao Z, Zhang S, et al. A biocompatible electrolyte enables highly reversible Zn anode for zinc ion battery. *Nat Commun*. 2023;14:6526.
62. Meng X, Zhou S, Li J, et al. Regulated ion-conductive electrode-electrolyte interface by in situ gelation for stable zinc metal anode. *Adv Funct Mater*. 2023:2309350.
63. Shin KH, Ji D, Park JM, et al. Structural composite hydrogel electrolytes for flexible and durable Zn metal batteries. *Adv Funct Mater*. 2023;34:2309048.
64. Yang H, Chang Z, Qiao Y, et al. Constructing a super-saturated electrolyte front surface for stable rechargeable aqueous zinc batteries. *Angew Chem Int Ed.* 2020;59: 9377–9381.
65. Guo C, Zhou J, Chen Y, et al. Synergistic manipulation of hydrogen evolution and zinc ion flux in metal-covalent organic frameworks for dendrite-free Zn-based aqueous batteries. *Angew Chem Int Ed.* 2022;61:e202210871.
66. Xin W, Xiao J, Li J, et al. Metal-organic frameworks with carboxyl functionalized channels as multifunctional ion-conductive interphase for highly reversible Zn anode. *Energy Storage Mater*. 2023;56:76–86.
67. Yang H, Qiao Y, Chang Z, et al. Reducing water activity by zeolite molecular sieve membrane for long-life rechargeable zinc battery. *Adv Mater.* 2021;33:2102415.
68. Zhu J, Bie Z, Cai X, et al. A molecular-sieve electrolyte membrane enables separator-free zinc batteries with ultralong cycle life. *Adv Mater.* 2022;34:2207209.
69. Xu J, Han P, Jin Y, et al. Hybrid molecular sieve-based interfacial layer with physical confinement and desolvation effect for dendrite-free zinc metal anodes. *ACS Nano*. 2024;18:18592–18603.
70. Deng C, Xie X, Han J, et al. A sieve-functional and uniform-porous kaolin layer toward stable zinc metal anode. *Adv Funct Mater*. 2020;30:2000599.
71. Guo R, Liu X, Xia F, et al. Large-scale integration of a zinc metasilicate interface layer guiding well-regulated Zn deposition. *Adv Mater.* 2022;34:2202188.
72. Xu D, Ren X, Xu Y, et al. Highly stable aqueous zinc metal batteries enabled by an ultrathin crack-free hydrophobic layer with rigid sub-nanochannels. *Adv Sci*. 2023; 10:2303773.
73. Wang L, Zhang B, Zhou W, et al. Tandem chemistry with Janus mesopores accelerator for efficient aqueous batteries. *J Am Chem Soc*. 2024;146:6199–6208.
74. Jiang Z, Du Z, Pan R, et al. Electrosynthesis of metal-organic framework interlayer to realize highly stable and kinetics-enhanced Zn metal anode. *Adv Energy Mater*. 2024: 2402150.
75. Zong Q, Lv B, Liu C, et al. Dendrite-free and highly stable Zn metal anode with $BaTiO_3$/P(VDF-TrFE) coating. *ACS Energy Lett*. 2023;8:2886–2896.
76. Zhou S, Meng X, Fu C, et al. Aligned dipoles induced electric-field promoting zinc-ion de-solvation toward highly stable dendrite-free zinc-metal batteries. *Small*. 2023;19: e2303457.
77. So S, Ahn YN, Ko J, et al. Uniform and oriented zinc deposition induced by artificial Nb_2O_5 Layer for highly reversible Zn anode in aqueous zinc ion batteries. *Energy Storage Mater*. 2022;52:40–51.
78. Yang H, Wang J, Zhang P, et al. Dielectric-ion-conductive $ZnNb_2O_6$ layer enabling rapid desolvation and diffusion for dendrite-free Zn metal batteries. *J Energy Chem*. 2025;100:693–701.
79. Yang Z, Lai F, Mao Q, et al. Reversing zincophobic/hydrophilic nature of metal-N-C via metal-coordination interaction for dendrite-free Zn anode with high depth-of-discharge. *Adv Mater*. 2024;36:2311637.
80. Chen S, Chen J, Liao X, et al. Enabling low-temperature and high-rate Zn metal batteries by activating Zn nucleation with single-atomic sites. *ACS Energy Lett*. 2022; 7:4028–4035.
81. Zhang W, Yao Q, Wang C, et al. Taming Zn electrochemistry with carbon nitride: atomically gradient interphase for highly reversible aqueous Zn batteries. *Adv Funct Mater*. 2023;34:2303590.

Xiaomin Cheng obtained her Ph.D. degree from East China University of Science and Technology in 2023. Since 2023, she works as a postdoctoral researcher at Suzhou Institute of Nano-Tech and Nano-Bionics under the supervisions of Prof. Hongzhen Lin. She is currently working on the application of new-type battery systems.

Yongzheng Zhang received his Ph.D. degree from East China University of Science and Technology (ECUST) in 2019. Since 2019, he works as a postdoctoral researcher at Beihang University and ECUST under the supervisions of Prof. Shubin Yang and Prof. Licheng Ling, respectively. His current research interests mainly focus on the 2D electrocatalysts for aqueous zinc-ion batteries and lithium-sulfur batteries.

Jian Wang is currently a research fellow supported by Alexander von Humboldt foundation in Helmholtz Institute Ulm (HIU) and Karlsruhe Institute of Technology (KIT) after receiving his Ph.D. degree from University of Science and Technology of China. His research interests focus on the applications of catalysis in secondary batteries ("Catalysis-in-Batteries") and the exploration of in-situ characterizations for probing catalytic mechanisms.

Hongzhen Lin is a senior researcher at i-lab of Suzhou Institute of Nano-Tech and Nano-bionics, Chinese Academy of Sciences, and University of Science and Technology of China. He majors in developing high energy density lithium metal-based energy storage systems with catalytic functionalities and their in-situ interfacial nonlinear spectroscopy characterization.